ORIGINAL ARTICLE

Skeleton in the closet: hidden diversity in patterns of cranial and postcranial ontogeny in Neotropical direct-developing frogs (Anura: Brachycephaloidea)

Florencia Vera Candioti[1] · Javier Goldberg[2] · Mauricio S. Akmentins[3] · Paulo Nogueira Costa[4] ·
Pedro Paulo Goulart Taucce[5] · José Pombal Jr[6]

Abstract

Direct development implies transformations with respect to the anuran biphasic life cycle, including changes in embryonic anatomy. In the clade Brachycephaloidea, skeletal ontogeny is known in *Eleutherodactylus coqui* of the basal family Eleutherodactylidae. In this work, we study it in four species representing the two other families in the group. We worked with developmental series of *Oreobates barituensis*, *Haddadus binotatus*, *Ischnocnema henselii*, and *Brachycephalus ephippium*. Specimens were prepared following protocols of clearing and staining and histology. In the cranium, results show an overall shared pattern that, as summarized for *E. coqui*, combines a partial recapitulation of aspects of the ancestral biphasic ontogeny with a profound remodeling that includes lost/novel structures and heterochronic shifts of developmental events. Among these transformations are the absence of suprarostrals and trabecular horns and the precocious ossification of jaw and suspensorium. In addition, each lineage shows particular features such that skull ontogeny varies interspecifically. In turn, the morphogenesis of the axial and appendicular skeleton is highly conserved, with main variations including the extent of ossification at hatching. Along with some external features such as the egg tooth and the enveloping tail with transversely arranged fins, an ossification sequence with extremely accelerated ossification of jaws and suspensorium could be distinctive of Brachycephaloidea.

Keywords *Brachycephalus* · *Haddadus* · Heterochrony · *Ischnocnema* · *Oreobates*

✉ Florencia Vera Candioti
   florivc@gmail.com

[1] Unidad Ejecutora Lillo, Consejo Nacional de Investigaciones Científicas y Técnicas – Fundación Miguel Lillo, San Miguel de Tucumán, Tucumán, Argentina

[2] Instituto de Bio y Geociencias del NOA, Consejo Nacional de Investigaciones Científicas y Técnicas, Rosario de Lerma, Salta, Argentina

[3] Instituto de Ecorregiones Andinas, Consejo Nacional de Investigaciones Científicas y Técnicas, Universidad Nacional de Jujuy, San Salvador de Jujuy, Jujuy, Argentina

[4] Museu de Biodiversidade Tauari, Universidade Federal do Sul e Sudeste do Pará, Marabá, Pará, Brazil

[5] Departamento de Biodiversidade e Centro de Aquicultura, Instituto de Biociências, Universidade Estadual Paulista, Câmpus Rio Claro, Rio Claro, São Paulo, Brazil

[6] Departamento de Vertebrados, Museu Nacional, Universidade Federal do Rio de Janeiro, Rio de Janeiro, Rio de Janeiro, Brazil

Introduction

Anurans are known to have an enormous variety of reproductive and developmental modes, including several that deviate from the plesiomorphic biphasic life cycle characterized by the larval stage—metamorphosis—adult stage progression (e.g., Haddad and Prado 2005). Among these, direct development is characterized by the lack of a free-living larval phase and an ontogenetic trajectory from embryos to terrestrial posthatching stages sustained exclusively from the yolk supplied in the egg (Thibaudeau and Altig 1999). This developmental mode, reported in at least 8 independent frog lineages, implies substantial modifications to the biphasic life cycle, involving also major changes in embryonic anatomy (e.g., Townsend and Stewart 1985). While several studies survey main developmental changes concerning external morphology (a recent review in Schweiger et al. 2017), the ontogeny of the skeletal system and how it differs from the well-known metamorphic transformations from tadpole to adult skeleton are scarcely explored.

GfBS

Springer

The large Neotropical clade Brachycephaloidea includes more than a thousand species likely all characterized by having direct development (Padial et al. 2014). Studies on early ontogeny of these species have gained a renewed interest following deep taxonomic rearrangements of what used to be the large "*Eleutherodactylus*" genus (e.g., Nokhbatolfoghahai et al. 2010; de Lima et al. 2016). In this work, we study the skeletal development of four brachycephaloid species, representing four genera and two of the three families it currently recognizes (Padial et al. 2014). *Oreobates* and *Haddadus* belong to two of the three subfamilies of Craugastoridae, Holoadeninae and Craugastorinae, respectively. In previous contributions, we described ontogenetic transformations in external characters of *Oreobates barituensis* and *Haddadus binotatus* (Goldberg et al. 2012; Goldberg and Vera Candioti 2015) and discussed their distinct features related to direct development. *Ischnocnema* and *Brachycephalus* are the only two genera of the family Brachycephalidae. We have recently studied the early ontogeny of *Ischnocnema henselii*, including skin and thyroid gland development (Goldberg et al. 2020). The unique features of the hyperossified cranial and postcranial skeleton of *Brachycephalus* species have been known since about two centuries (e.g., Cocteau 1835; Miranda-Ribeiro 1920; Goutte et al. 2019), and the examination of developmental patterns that lead to that extraordinary morphology is of interest to interpret extents of bone fusions/losses as related to miniaturization in the genus (e.g., Trueb and Alberch 1985). Hence, we also include in our study the single ontogenetic series available for the genus, a collection of a few embryos of *Brachycephalus ephippium* preserved after the study by Pombal Jr. (1999). Finally, the third brachycephaloid family Eleutherodactylidae includes the widely studied *Eleutherodactylus coqui*, and the large amount of literature available for this species will be used to compare and discuss skeletal ontogenetic patterns in direct-developing frogs.

Material and methods

We studied developmental series of *Brachycephalus ephippium* ($N = 2$), *Ischnocnema henselii* ($N = 4$), *Haddadus binotatus* ($N = 6$), and *Oreobates barituensis* ($N = 10$), consisting of embryos reared from clutches collected in the field and periodically preserved in buffered 10% formalin. Details of oviposition aspects and lab rearing are provided elsewhere for part of the material (Pombal Jr. 1999; Goldberg et al. 2012, 2020; Goldberg and Vera Candioti 2015). In addition, a new clutch of *O. barituensis* was obtained from the field (December 29, 2015; Ocloyas, Jujuy, Argentina; 23° 58′ 29.10″ S, 65° 14′ 45.40″ O, 1540 m asl), and embryos were euthanized and preserved every 8–12 h. Most specimens were prepared in toto following a clearing

and staining protocol (Wassersug 1976), and two individuals of all species were prepared for serial sectioning and routine histological staining. Embryos were staged following Townsend and Stewart (1985); further details of the material examined are summarized in Table 1.

Results

Detailed descriptions of cranial and postcranial development are given for *Oreobates barituensis*, and development of the other three species is described consigning main differences. Unfortunately, the series of *Brachycephalus ephippium* is very incomplete; thus, descriptions are provided only for two specimens. Figures 1, 2, 3, 4, 5, 6, 7, 8, 9, 10, 11, 12, and 13 show main aspects described in the text for all species, and Tables 2, 3, and 4 summarize sequences of chondrification and ossification both for cranial and postcranial elements.

Oreobates barituensis

Cranial ontogeny At TS10, cranial trabeculae are visible as rod-like cartilages located ventrolateral to the brain. They are united posteriorly by the future basal plate, and they approach one another rostrally. In the olfactory region, only the solum, tectum, and septum nasi are developed. A thin pila antotica ascends dorsally from each trabecula; the pila metoptica begins to develop as a small bump rostral to the pila antotica. The trabecular horns and suprarostral cartilages never form. The otic capsules are large (44% of the cranium length) and rounded. The palatoquadrate is very thin, weakly Alcianophilic, not connected to the neurocranium, and oriented at an angle of 30° relative to its anteroposterior axis. The lower jaw has an inverted U-shape. The medial region corresponds to the infrarostral cartilages, which are medially fused through a thick symphysis; Meckel's cartilages are thin, curved caudally, and reach the plane of the pila metoptica; they are fully fused to the infrarostral cartilages forming a single rod of cartilage. In the hyobranchial skeleton, the ceratohyals already resemble the hyale of metamorphic stages; they are long, with similar width along their entire length, and curve posteriorly; the anterior processes are short and stout. Unfortunately, Alcian blue staining was too weak for us to resolve ceratobranchial configuration.

At TS11–12 (Fig. 1a), the skull is completely cartilaginous. The developing nasal capsules include inferior prenasal cartilages, planum antorbitale, antorbital process, and planum triangulare. The pila antotica and pila metoptica extend dorsally and are connected to each other through cartilaginous bridges. The orbital cartilage begins to develop completing the lateral walls of the cranium. In the otic region, an operculum is already developed and a thin tectum synoticum projects

Table 1 Material examined. Developmental stages follow Townsend and Stewart (1985)

	Cleared and stained	Serial sections	Acronyms
Oreobates barituensis			
TS10	1		IBIGEO 1363 (material from Goldberg et al. 2012)
TS11–12	1		MSA 271
TS12	1	1	IBIGEO 1363 (material from Goldberg et al. 2012)
TS13	1		MSA 271
TS14	1		MSA 271
TS15 (whole tail)	1		MSA 271
Hatchling	2	1	IBIGEO 1363 (material from Goldberg et al. 2012); MSA 271
Haddadus binotatus			
TS12	1	1	MNRJ 86848 (material from Goldberg and
TS13	1		Vera Candioti 2015)
TS14	1		
TS15	1		
Hatchling		1	
Ischnocnema henselii			
TS11–12	1		CFBH 39509 (material from Goldberg et al. 2020)
TS13		1	
TS14		1	
Hatchling	1		
Brachycephalus ephippium			
TS13	1	1*	FML 30775 (material from Pombal Jr. 1999)
TS15	1	1*	

CFBH, amphibian collection of Célio F. B. Haddad, Departamento de Zoologia, Instituto de Biociências, Universidade Estadual Paulista, Campus de Rio Claro, São Paulo; *FML*, herpetological collection of Fundación Miguel Lillo; *IBIGEO*, Instituto de Bio y Geociencias del NOA, CONICET; *MSA*, collection of Mauricio S. Akmentins; *MNRJ*, Museu Nacional, Universidade Federal do Rio de Janeiro, Rio de Janeiro

*The same cleared and stained specimen was later sectioned

medially from the dorsal aspect of each otic capsule. The palatoquadrate cartilage is short and oriented at an angle of 45° relative to the anteroposterior axis of the neurocranium; it is not attached to the neurocranium. The articular process is stout and articulates with Meckel's cartilage, whereas the posterior extreme is thin and does not reach the otic capsule. The pterygoid process is stout and long and directed rostrally reaching almost the anterior margin of the orbit; caudal to the pterygoid process, the palatoquadrate becomes slightly taller, likely representing a much reduced muscular process. In the lower jaw, Meckel's cartilages have grown longer to reach the pila antotica. The hyobranchial skeleton (Fig. 1b) has a weak hypobranchial plate; the hyale are curved and have more prominent anterior processes. Ceratobranchials I are still distinct, long and thin, and ceratobranchials II are fully reduced to small processes on the lateral margins of the hypobranchial plate; posterior processes are thin, short, and divergent. No ossifications are evident in whole-mount preparations, but histological sections reveal angulosplenials developing on the ventral aspect of Meckel's cartilage.

At TS13, the palatoquadrate is visible as a thin, cartilaginous structure oriented at an angle of about 55° relative to the anteroposterior axis of the neurocranium. The dorsal extreme is the otic process that approaches the anterolateral region of the otic capsule; the ventral extreme is the articular process that articulates with the posterior edge of Meckel's cartilage. Maxillary and pterygoid processes join at this stage. In the hyobranchial apparatus, the ceratobranchials I are fully reduced, and small anterolateral processes remain instead. Ossifications of the angulosplenials and squamosals are present, and a slight coloration indicates the beginning of differentiation of the maxillae in the upper jaw.

At TS14, the cartilaginous skeleton undergoes further changes in the nasal region. Alary, oblique, superior and inferior prenasal cartilages, subnasal crest, lateral commissures, and the laminae superior and inferior (which delimit principal, medial, and inferior nasal cavities) are differentiated (Fig. 2). Posteriorly, a thin planum antorbitale is visible, with a long, ventrally oriented antorbital process; a short and weak maxillary anterior process; and a long, posterior pterygoid process.

Table 2 Developmental events during cranial chondrogenesis in terraranan species. A reference for colors is given; dark colors show early development of structures, whereas lighter colors are indicative of delayed differentiation. Data for *Eleutherodactylus coqui* are obtained from Hanken et al. (1992). In the species we examined, the darkest colors correspond to the earliest specimens available; thus, the true first differentiation of some structures is surely underestimated; a symbol (−) indicates events that, if present, occurred necessarily earlier. Symbol (?) indicates uncertain information (i.e., unclear observations or presumable data), and (*) highlights hatched specimens

	Ec	Be	Ih	Hb	Ob
Palatoquadrate 30°		-	-	-	
Septum and tectum nasi					
Planum antorbitale					
Solum nasi					
Pterygoid-maxillary processes					
Palatoquadrate 45°			-		
Planum terminale		?			
Hyoid anterior process					
Alary and oblique cartilages					
Prenasal cartilages					
Four ceratobranchials until		-	-		?
Ceratobranchials I until		-			
Palatoquadrate-otic capsule					
Pseudobasal processes		?	*		*
Hyoid anterolateral processes		?			
Palatoquadrate 90°		hatching?			
Inferior and superior laminae	?				
Hyoid final configuration					

Legend:
< TS8-9
> TS10
> TS11
> TS12
> TS13
> TS14
> TS15
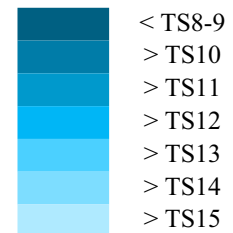
Ec, *Eleutherodactylus coqui*; Be, *Brachycephalus ephippium*; Ih, *Ischnocnema henselii*; Hb, *Haddadus binotatus*; Ob, *Oreobates barituensis*

Premaxillae and small dentaries ossify. Meckel's cartilages become thinner and longer and extend to almost the posterior end of the otic capsules. The palatoquadrate cartilages acquire a perpendicular arrangement regarding the neurocranium axis.

At TS15 (Fig. 3), the cranium is still almost completely cartilaginous. In the cranial roof, the taenia tecti transversalis grows from the taenia tecti marginales, and a small taenia tecti medialis develops from the anterior margin of the tectum synoticum (Fig. 3a). The jaw suspension is located ventral and anterior to the otic capsules. The dorsal otic process is formed, and histological sections of a hatched specimen show an additional, stout pseudobasal process. The region corresponding to infrarostral cartilages is very small and weak, and Meckel's cartilages are stout. The hyobranchial skeleton has almost the adult shape (Fig. 3b). The long anterior processes of the hyalia run parallel in rostral direction; the posterior extreme of each hyale is dorsally curved to reach close contact with the otic capsule. The hyoid plate is quadrangular and weakly chondrified; on its lateral margins, the antero- and posterolateral processes are outlined. Caudally, the posteromedial processes are long and divergent. Discrete ossifications at this stage are the premaxillae, maxillae, septomaxillae, and nasals (Fig. 3c), angulosplenials, dentaries, very thin pterygoids dorsal to the caudal edge of pterygoid processes (Fig. 3d), and squamosals with stout ventral and otic rami, and a small zygomatic ramus; frontoparietals are present as narrow slivers dorsal to the orbital cartilages.

Parasphenoid and prootics are slightly outlined on the ventral aspect of the cranium floor and the anterior surface of the otic capsules, respectively.

Postcranial ontogeny At TS10, the cartilaginous precursors of all eight presacral and the sacral vertebrae are present as paired condensations that develop dorsolaterally to the notochord. Anterior vertebrae appear more defined with atlas condensations wider than those of the other vertebrae. A small postsacral vertebra also develops at this stage, evident as a pair of condensations. By TS12, the neural arches primordia remain as paired condensations, although larger (Fig. 1c). Vertebrae II and III exhibit incipient, short transverse processes. Postsacral 2 appears as a pair of neural arch pedicels posterior to postsacral 1. Next, the transverse process of vertebra IV develops. All vertebrae present incipient postzygapophyses. Ossification begins with two bony centers on the cartilaginous centrum of the atlas. Ossification centers also occur in the dorsal half of the atlas pedicels and in the pedicels of all presacral vertebrae underneath transverse processes. At TS13, the hypochord appears as a small cartilaginous bar at the level of the neural arches of the first postsacral vertebra, parallel and ventral to the notochord. At TS14–15, the neural arch laminae of all presacral vertebrae are expanded medially (Fig. 4a). Vertebrae II–VIII have well-defined, although small, transverse processes (III > II > IV > V = VI = VII = VIII). All presacral vertebrae bear small pre- (except the atlas) and

Table 3 Developmental events during limb chondrogenesis in terraranan species. A reference for colors is given; dark colors show early development of structures, whereas lighter colors are indicative of delayed differentiation. Data for *E. coqui* are obtained from Hanken et al. (2001). In the species we examined, the darkest colors correspond to the earliest specimens available; thus, the true first differentiation of some structures is surely underestimated; a symbol (−) indicates events that, if present, occurred necessarily earlier. Symbol (?) indicates uncertain information, and (*) highlights hatched specimens. Species references as in Table 1

	Ec	Be	Ih	Hb	Ob
(A) Forelimbs					
Humeri		-	-	-	
Radii		-	-	-	
Ulnae		-	-	-	
Radialia		-	-	-	
Carpal distalia 4-5					
Carpal distalia 3					
Metacarpalia III-V					
Proximal phalanges IV-V					
Carpal distalia 2					
Elements Y					
Metacarpalia II					
Middle phalanges IV					
Proximal phalanges III					
Middle phalanges V		absent			
Terminal phalanges V		absent			
Terminal phalanges IV					
Terminal phalanges III					
Proximal phalanges II					
Prepollices	?		?		
Terminal phalanges II		absent			
(B) Hind limbs					
Femora		-	-	-	
Tibia-fibulae		-	-	-	
Tibiale-fibularia		-	-	-	
Tarsal distalia 3-2			-	-	
Metatarsalia II-V					
Proximal phalanges V		hatching?			
Proximal phalanges IV					
Proximal phalanges III					
Metatarsalia I					
Mid-proximal phalanges IV					
Proximal phalanges II					
Mid-distal phalanges IV					
Middle phalanges V		absent?			
Elements Y		?			
Terminal phalanges IV-V		absent			
Prehalluces		hatching?			
Tarsal distalia 1					
Middle phalanges III					
Terminal phalanges II-III		hatching?			
Proximal phalanges I					
Terminal phalanges I		absent			

Color legend: < TS8-9; > TS10; > TS11; > TS12; > TS13; > TS14; > TS15

postzygapophyses; the postzygapophyses of presacral vertebrae I–VI seem to articulate with the prezygapophyses. The sacrum bears a pair of small rounded diapophyses. At hatching, both counterparts of the postsacral vertebra 1 remain separated and each side has an anterior cotyle, whereas both halves of postsacral vertebra 2 are well differentiated. An additional cartilaginous growth of the posterior margin of postsacral vertebra 2 suggests the development of a third

Table 4 Ossification of individual bones in terraranan species. Ossification in *Eleutherodactylus* is taken from Hanken et al. (1992; skull—*E. coqui*), Hanken et al. (2001; limbs—*E. coqui*), and Meza-Joya et al. (2013; column—*E. johnstonei*); further data about postcranial ossification are not available in the literature. In the species we examined, the darkest colors correspond to the earliest specimens available; thus, the true first ossification of some structures is surely underestimated; a symbol (−) indicates events that, if present, occurred necessarily earlier. Symbol (?) indicates uncertain observations, and (*) highlights hatched specimens. Species references as in Table 1

	E	Be	Ih	Hb	Ob
(A) Cranium					
Angulosplenials					
Squamosals					
Premaxillae					
Parasphenoid					
Maxillae					
Frontoparietals					
Pterygoids					
Dentaries					
Exoccipitals			?		
Mentomeckelians		?			
Quadratojugals		absent	*		
Septomaxillae		?	*		
Nasals		?			
Prootics			*		
Vomers		?	*		
Hyoid posterior processes		?	*		
Neopalatines		absent	*	*	
Sphenethmoid		?			
(B) Postcranium					
Scapulae					
Ilia					
Humeri				-	
Femora				-	
Radius-ulnae					
Tibia-fibulae				-	
Tibiale-fibularia	-	?			
Metatarsalia	-	IV?	III-V	III-IV	III-V
Transverse processes					
Coracoids			?		
Metacarpalia		III-IV?	?	II-V	III-V
Ischia			*		
Clavicles		?			
Cleithra		?			
FL Proximal phalanges		?	?	II-V	IV
HL Proximal phalanges	-	?	?	III-V	IV-V
Hypochord		?	*		*
Suprascapulae		?	*	?	?
FL Terminal phalanges		?	*II-V	II-V	III-V
HL Terminal phalanges		?	*I-V	I-V	II-V
Epicoracoids		?			
Distal carpalia		?			
Distal tarsalia	?	?			
Prepollices and prehalluces		?			

Legend:
- < TS12
- TS12-TS13
- > TS13
- > TS14
- > TS15
- after hatching
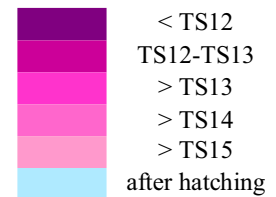
postsacral vertebra. Boundaries between the neural arch pedicels of postsacral vertebrae 1 and 2 and between those of postsacral vertebrae 2 and 3 are indicated by the presence of large foramina. Therefore, at hatching, both counterparts of the coccyx are present. Ossification of the hypochord is slightly noticeable at this stage.
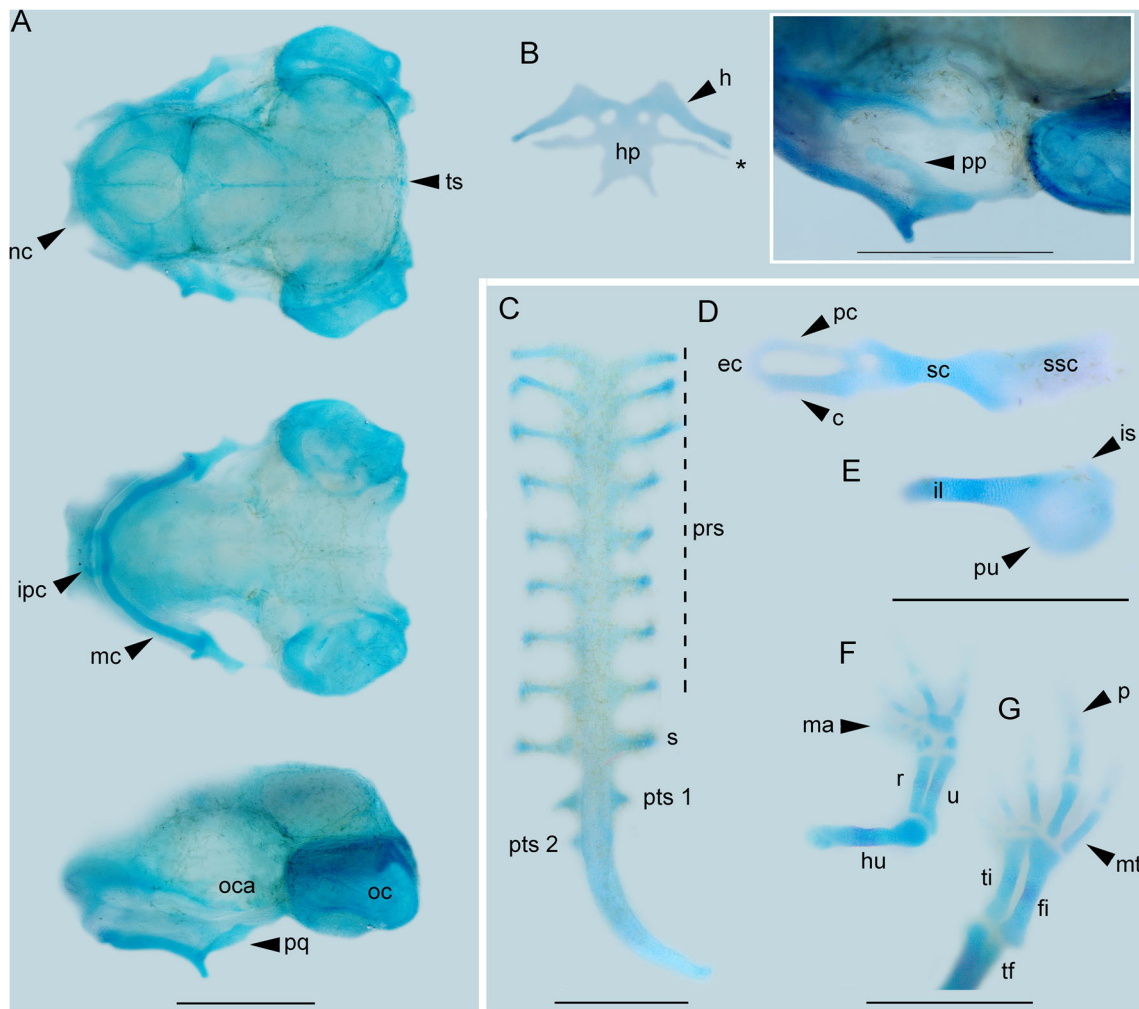
Fig. 1 Skeletal morphology of *Oreobates barituensis* at TS12. **a** Skull dorsal, ventral, and lateral views. **b** Hyobranchial apparatus, ventral view. *Inset:* detail of the palatoquadrate cartilage with a long pterygoid process. **c** Vertebral column, dorsal view. **d** Pectoral girdle, ventral view. **e** Pelvic girdle, lateral view. **f** Forelimb, dorsal view. **g** Hind limb, dorsal view. *Abbreviations*: *c*, coracoid; *ec*, epicoracoid; *fi*, fibulare; *h*, hyale; *hp*, hypobranchial plate; *hu*, humerus; *il*, ilium; *ipc*, inferior prenasal cartilage; *is*, ischium; *ma*, manus; *mc*, Meckel's cartilage; *mt*, metatarsalia; *nc*, nasal capsule; *oc*, otic capsule; *oca*, orbital cartilage; *p*, phalanges; *pc*, procoracoid; *pp*, pterygoid process; *pq*, palatoquadrate; *prs*, presacral vertebrae; *pts*, postsacral vertebra; *pu*, pubis; *r*, radius; *s*, sacrum; *sc*, scapula; *ssc*, suprascapula; *tf*, tibia–fibula; *ti*, tibiale; *ts*, tectum synoticum; *u*, ulna. The asterisk shows the remaining ceratobranchial I in the hyobranchial skeleton. *Scale bars* = 1 mm

In the pectoral girdle, at TS10, each half is composed of two cartilaginous primordia that correspond to the scapula and the coracoid. By TS12, the procoracoid cartilage is differentiated and it fuses with the scapula and coracoid to define the glenoid fossa (Fig. 1d). The suprascapular cartilage appears as a flat sheath next to the scapula. By TS13, the epicoracoid is fully formed forming the cartilaginous bridge between the coracoid and the procoracoid. The endochondral ossification of the coracoid and scapula occurs earlier than the dermal ossification of the clavicle and the cleithrum (Fig. 4b). Mineralization of the suprascapulae is evident from TS14. Sternum elements are not differentiated in prehatching stages.

Forelimb development is depicted in Figs. 1f and 4d and summarized in Fig. 5a. At TS10, the first elements to appear are those related to the primary axis, i.e., the ulnare, distal carpale 5-4, and finger IV. The preaxial process of the ulnare (interpreted as the cartilage intermedium by Fabrezi and Barg 2001) is present at this stage. The radiale and the element Y are formed by the secondary fusions of two embryonic condensations each. The last fusion of carpal elements (distal carpale 5-4 plus distal carpale 3) begins at TS12. An unidentified condensation appears postaxially and close to the distal end of the ulna. Fusion of radius and ulna begins at their proximal ends by TS13, simultaneously with the fusion of condensations forming the element Y and the radiale. By TS14, the proximal element of prepollex and the terminal phalanges of fingers III–V differentiate. The ossification begins after TS10 and occurs proximodistally and preaxially. Before hatching, diaphyses of all long bones (humerus, radioulna, metacarpalia, and phalanges) are ossified.
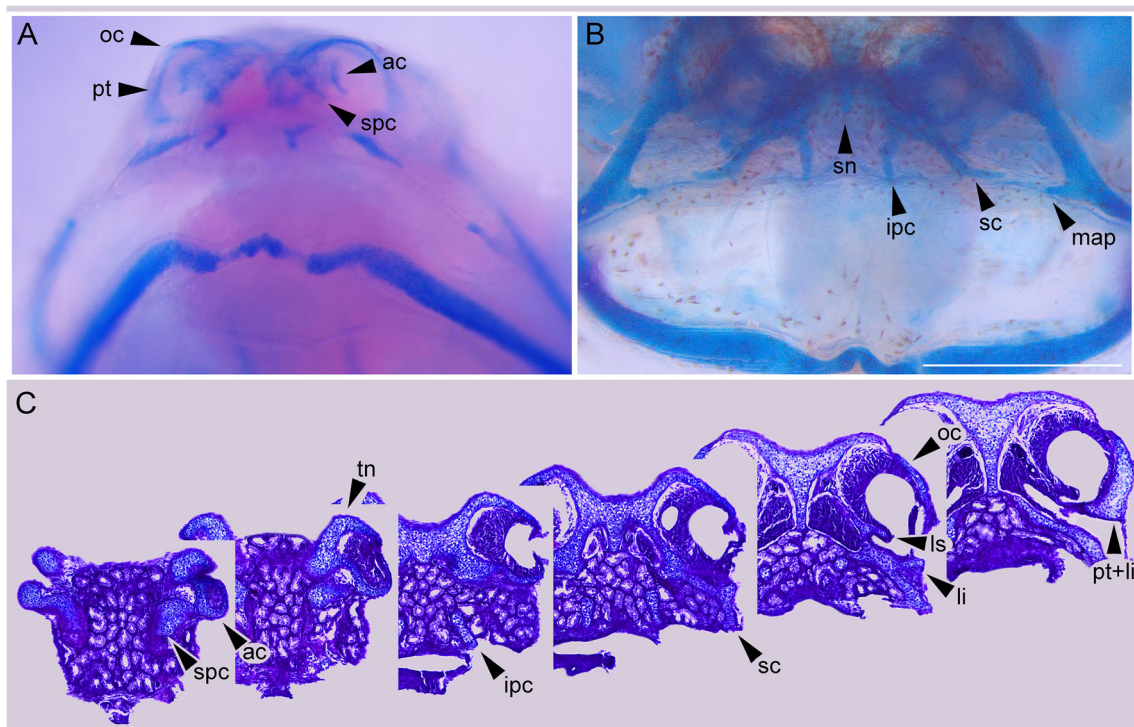
Fig. 2 Development of the nasal region of *Oreobates barituensis*. **a** TS14, anteroventral view of the snout. **b** Hatchling, frontal view of the snout. **c** Hatchling, serial sections of the nasal region; hematoxylin–eosin staining; nonconsecutive images were selected in order to show main nasal structures, from front (first, left image) to caudal region (last image).

Abbreviations: *ac*, alary cartilage; *ipc*, inferior prenasal cartilage; *li*, lamina inferior; *ls*, lamina superior; *map*, maxillary anterior process; *oc*, oblique cartilage; *pt*, planum terminale; *sc*, subnasal crest; *sn*, septum nasi; *spc*, superior prenasal cartilage; *tn*, tectum nasi. *Scale bars* = 1 mm (**a**, **b**) and 0.1 mm (**c**)

Regarding the pelvic girdle, at TS10, the first elements to appear are the ilia and the pubes as two independent cartilaginous condensations on each side of the girdle, at the level of the first postsacral vertebra. As development progresses, ilia elongate anteriorly. Condensations of the ischia appear and migrate toward each other and fuse to form, together with the medially attached pubes, the acetabula. As ilia elongate, ossification begins from a center near the midpoint of their shafts by TS12 (Fig. 1e). Before hatching, ossification of ilial shafts spreads anteriorly and posteriorly reaching the acetabula, while the ischia show the first signs of ossification in their posterior margins. Ilia attach to the developing sacral diapophyses by thin ligaments.

Hind limb development is slightly faster than that of the forelimbs (Figs. 1g, 4e, and 5b). At TS10, postaxial dominance of the primary axis is evident with the early differentiation of the proximal phalanx of toe IV. By TS12, three condensations are distinct in the tarsus, distal to the enlarged proximal tarsalia (fibulare and tibiale): the distal tarsale 3-2 (primary fusion), distal tarsal 1, and two condensations of the element Y. This latter acquires its definitive configuration at TS13, via the fusion of both primary independent condensations. Concomitant with this, the proximal element of the prehallux arises as a single condensation. At TS14, terminal phalanges are differentiated. Ossification begins before TS12,

earlier than the ossification in the manus, and it takes place in a proximodistal and postaxial–preaxial direction as well. All diaphyses of metatarsals and phalanges are ossified before hatching. Distal tarsal bones remain cartilaginous at hatching, and the distal prehallical element is still cartilaginous in adult specimens. The T-shape of terminal phalanges of toes and fingers is acquired after hatching.

Haddadus binotatus

Cranial ontogeny At TS12, the cartilaginous cranial skeleton in this species is similar to that of *Oreobates* (Fig. 6a). Conversely, hyobranchial skeleton development is delayed, with the ceratohyals showing a metamorphosed hyale-like shape, but larval ceratobranchials I–IV still differentiated (Fig. 6b). The ceratobranchials I are the longest, stout, and slightly curved posteriorly, whereas ceratobranchials II–IV are thinner and oriented laterally. Unlike in *Oreobates*, angulosplenials and squamosals appear ossified both in histological and whole-mount preparations. At TS13, palatoquadrate acquires a perpendicular disposition relative to the neurocranial axis, and further ossifications appear, i.e., the frontoparietals, parasphenoid, premaxillae, and maxillae, plus slightly outlined exoccipitals. The nasal region is comparatively more developed than in *O. barituensis*. Cranial
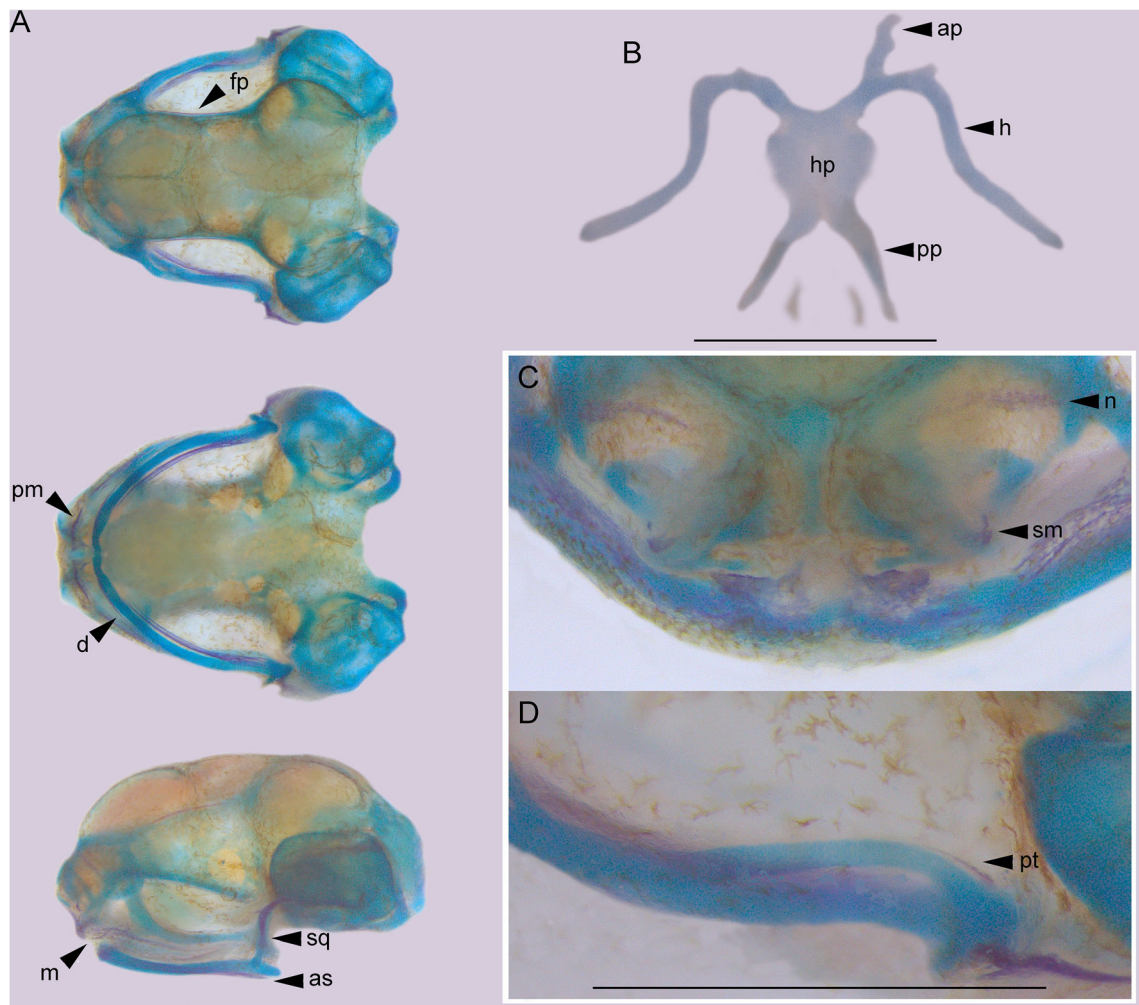
Fig. 3 Cranial skeleton of *Oreobates barituensis* at TS15. **a** Skull in dorsal, ventral, and lateral views. **b** Hyobranchial apparatus, ventral view. **c** Detail of the rostral region, dorsal view. **d** Detail of the caudal portion of the pterygoid process, dorsal view. Skull ossifications present at this stage are indicated. *Abbreviations*: *ap*, anterior process; *as*, angulosplenial; *d*, dentary; *fp*, frontoparietal; *h*, hyale; *hp*, hyoid plate; *m*, maxilla; *n*, nasal; *pm*, premaxilla; *pp*, posterior process; *pt*, pterygoid; *sm*, septomaxilla; *sq*, squamosal. *Scale bars* = 1 mm
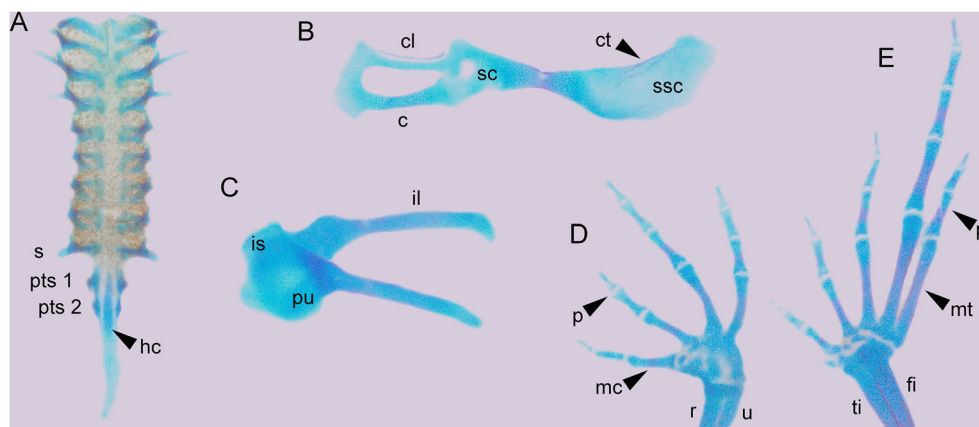
Fig. 4 Postcranial skeleton of *Oreobates barituensis* at TS15. **a** Vertebral column, dorsal view. **b** Pectoral girdle, ventral view. **c** Pelvic girdle, lateral view. **d** Forelimb, dorsal view. **e** Hind limb, dorsal view. *Abbreviations*: *c*, coracoid; *cl*, clavicle; *ct*, cleithrum; *fi*, fibulare; *hc*, hypochord; *il*, ilium; *is*, ischium; *mc*, metacarpalia; *mt*, metatarsalia; *p*, phalanges; *pts*, postsacral vertebra; *pu*, pubis; *r*, radius; *s*, sacrum; *sc*, scapula; *ssc*, suprascapula; *ti*, tibiale; *u*, ulna. *Scale bars* = 1 mm

Fig. 5 Schematic representation of auto- and zeugopodium development in *Oreobates barituensis*. **a** Forelimb. **b** Hind limb. The adult configuration is shown at the left, and drawings at the right show the sequential ossification (black segments) of elements. *Abbreviations*: *fi*, fibulare; *mc*, metacarpalia; *mt*, metatarsalia; *p*, phalanges; *ph*, prehallux; *pp*, prepollex; *r*, radius; *ra*, radiale; *ti*, tibiale; *u*, ulna; *ul*, ulnare; *Y*, element Y; *1–5*, distal carpalia and tarsalia; *I–V*, fingers and toes
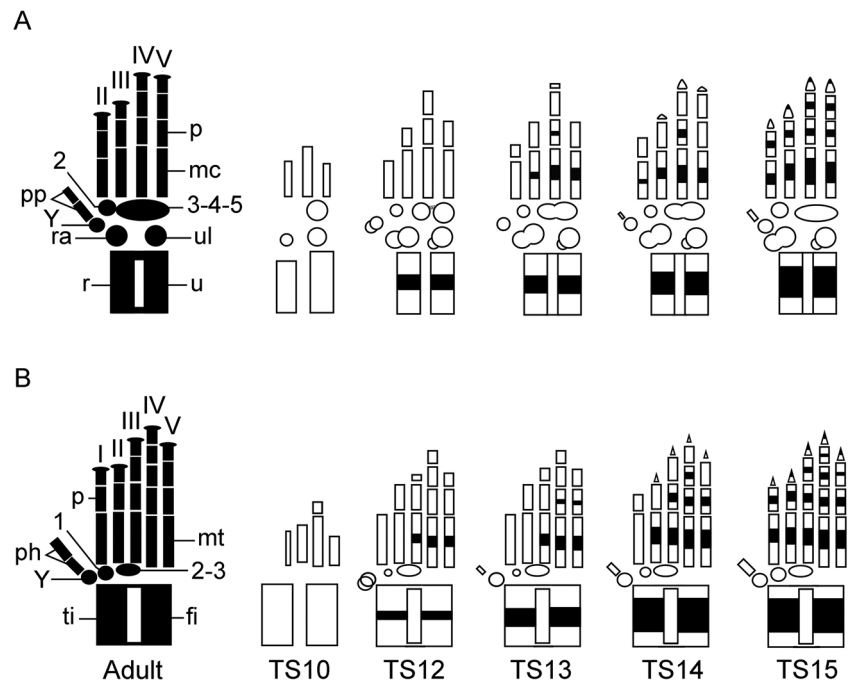
skeleton at TS14 appears adult-like, with a longer snout and overall more robust ossifications. Dentaries, pterygoids, and small quadratojugals differentiate at this stage. At TS15 (Fig. 7), the nasal region is prominent and developed, except for the lateral commissure between the oblique cartilage and the planum antorbitale which is still not completely formed. Further ossifications are the mentomeckelians (Fig. 7a), nasals and septomaxillae (Fig. 6b), vomers, prootics, and hyoid posterior processes. Maxillary teeth are present in the maxillae (Fig. 7a), and short zygomatic rami project rostrally in the squamosals (Fig. 7c). Serial sections of a hatched specimen show the neopalatines ossified.

Postcranial ontogeny The development of the axial skeleton is slightly faster than in *Oreobates*. Ossification of transverse processes begins at TS12 (Fig. 6c), and at TS13, all vertebrae appear well articulated and stronger. By TS14, the cartilaginous coccyx (postsacral elements 1 + 2) appears as a paired element and the hypochord begins to ossify. Finally, at TS15 (Fig. 8a), the prezygapophyses and postzygapophyses of all presacral vertebrae are cartilaginous but articulate with each other. The transverse processes are present in all presacral vertebrae, although larger in the anterior ones. The sacrum bears a pair of small, rounded diapophyses. The neural arch laminae of all vertebrae are fused at the midline and the regression of the notochord is visible caudally. In the pectoral girdle, clavicles begin to differentiate early at TS12 (Fig. 6d), and all bony elements, except the mineralized areas of the suprascapula, are already evident from TS13 (Fig. 8b). In turn, the pelvic girdle is more robust, with ischia slightly ossified and longer ilia with dorsal ridges already developed at TS14

(Figs. 6e and 8c). Limb chondrogenesis and ossification are faster than in *Oreobates*, with almost all elements ossified at TS14 (Figs. 6f, g; 8d, e; and 9). Further differences involve the ulnare formed by a single condensation and the differentiation of the distal element of the prepollex before hatching. Other than the overall accelerated development, there are no significant variations in tarsal configuration and ontogeny.

Ischnocnema henselii

Cranial ontogeny At TS11–12, the chondrocranium is slightly more advanced than those of *Oreobates* and *Haddadus* (Fig. 10a, b). Main differences are the more chondrified orbital cartilages, the almost perpendicular palatoquadrates, and in the hyobranchial skeleton, the differentiated anterior processes and completely reduced ceratobranchials. Nonossified anlagen of the angulosplenials and squamosals are outlined at this stage. At TS13, these ossified elements, plus the dentaries, maxillae, parasphenoid, and small premaxillae, are present in serial sections. Frontoparietals and pterygoids ossify at TS14. Finally, hatched specimens of *I. henselii* (Fig. 11) show almost all adult bones ossified, including the neopalatines (a difference regarding *Haddadus*), plus the mentomeckelians, quadratojugals, vomers, and hyoid posterior processes (differences regarding *Oreobates*); only the sphenethmoid differentiates at some point during juvenile stages.

Postcranial ontogeny Postcranial development is also faster than in the two previous species (Figs. 10c–g and 12). Fundamental differences with hatched specimens of the other species include a coccyx well developed although not fully
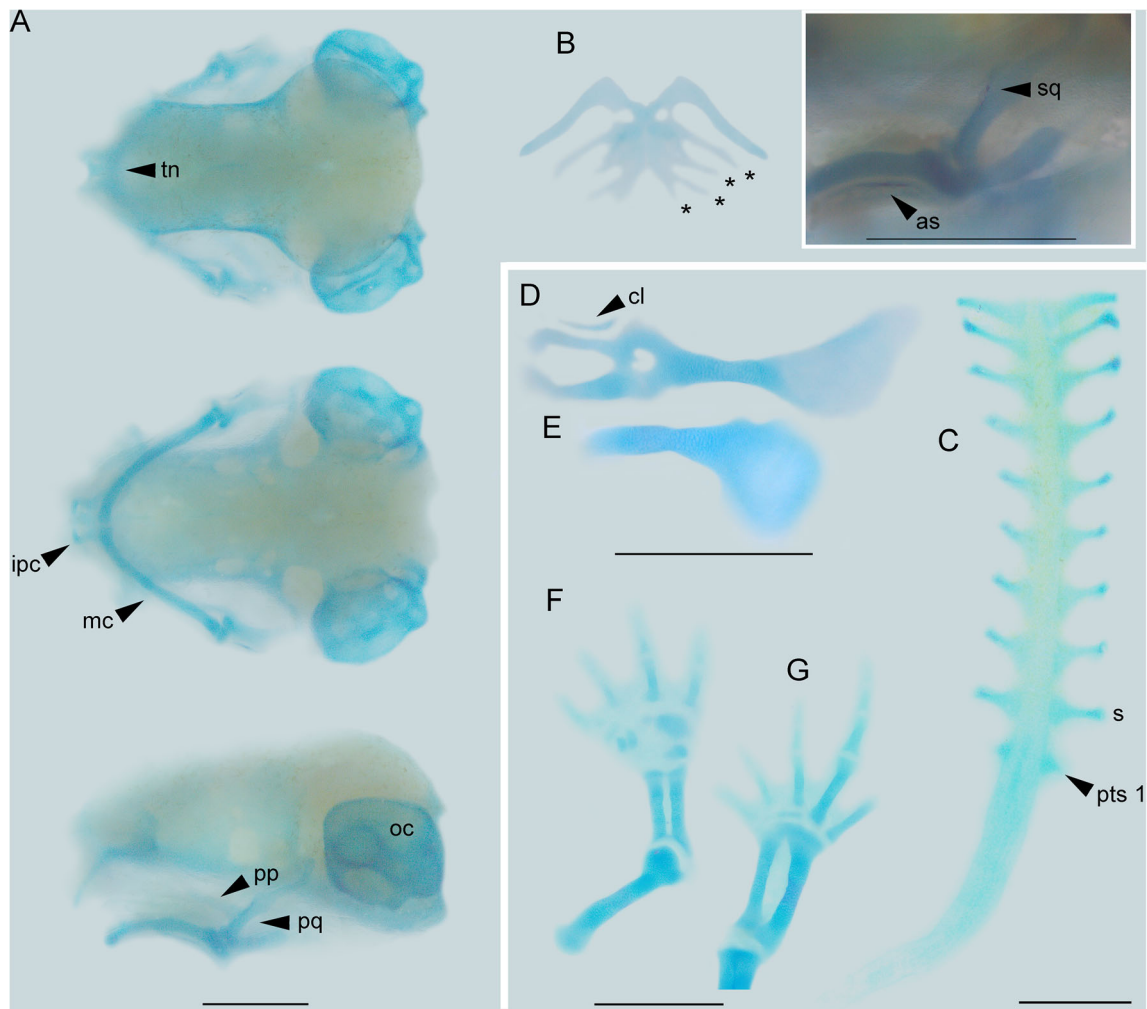
Fig. 6 Skeletal morphology of *Haddadus binotatus* at TS12. **a** Skull in dorsal, ventral, and lateral views. **b** Hyobranchial apparatus, ventral view. *Inset*: detail of the suspensorium region, showing the arrangement of the palatoquadrate and ossifications developed. **c** Vertebral column, dorsal view. **d** Pectoral girdle, ventral view. **e** Pelvic girdle, lateral view. **f** Forelimb, dorsal view. **g** Hind limb, dorsal view. *Abbreviations*: *as*, angulosplenial; *cl*, clavicle; *ipc*, inferior prenasal cartilage; *mc*, Meckel's cartilage; *oc*, otic capsule; *pp*, pterygoid process; *pq*, palatoquadrate; *pts*, postsacral vertebra; *s*, sacrum; *sq*, squamosal; *tn*, tectum nasi. The asterisks show the ceratobranchials I–IV still differentiated in the hyobranchial skeleton. *Scale bars* = 1 mm

ossified at hatching, a cartilaginous sternum already evident, and in the limbs, most bony elements, including the T-shaped terminal phalanges, differentiated; only the carpal bones remain cartilaginous. A single proximal prepollical element is discernible. Two prehallical cartilaginous elements are differentiated at hatching.

Brachycephalus ephippium

Cranial ontogeny At TS13, the nasal region is almost fully formed; only inferior and superior laminae are still not developed. All ceratobranchials are reduced, and hyoid has an adult-like aspect. Serial sections show ossification in angulosplenials and squamosals (Fig. 13a), dentaries, maxillae, and premaxillae; also, a light staining is outlined in the lateral parts of the frontoparietal region. At TS15 (Fig. 13b), the general aspect of

the chondrocranium appears underdeveloped in comparison with the three former species. The palatoquadrates do not reach their perpendicular arrangement regarding the neurocranium axis, and the rostral region is very short, more similar to early stages of other species. The nasal region is comparatively robust and well developed. Ossification is still weak, and in whole-mount preparation, only a thin calcified line is seen as evidence of still developing dentaries, angulosplenials, and squamosals; histological sections show slight ossification in pterygoids, parasphenoid, prootics, and exoccipitals.

Postcranial ontogeny Developmental series is unfortunately not complete enough for a detailed description of postcranial ontogeny, but some comparisons are possible. Main differences regarding the former species concern autopodium development. In hands, all elements except for some phalanges

Fig. 7 Cranial skeleton of *Haddadus binotatus* at TS15. **a** Skull in dorsal and ventral views. **b** Detail of the rostral region, frontal view. **c** Detail of the suspensorium region, showing ossifications in lateral view. *Abbreviations*: *as*, angulosplenial; *d*, dentary; *m*, maxilla; *mm*, mentomeckelian; *mt*, maxillary teeth; *n*, nasal; *oc*, otic capsule; *pm*, premaxilla; *qj*, quadratojugal; *sm*, septomaxilla; *sq*, squamosal. *Scale bars* = 1 mm
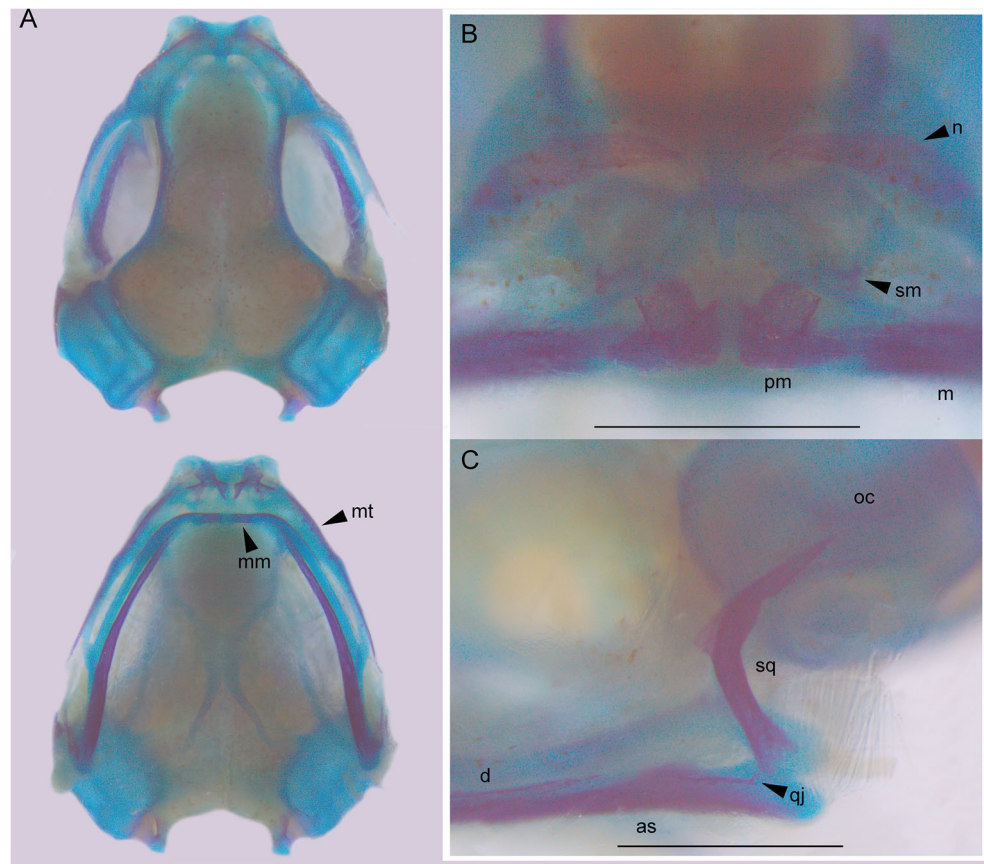
are evident at TS13. Finger III apparently completes its development before the proximal phalanx of finger V is formed. Likewise, toe II development precedes the formation of a complete toe V. Ossification is evident in vertebrae, proximal elements of the pectoral girdle, pelvic girdle, and long bones of limbs. At TS15, almost all limb elements are differentiated (e.g., Fig. 13b). Middle and terminal phalanges V and terminal phalanx II of the hand,

plus terminal (and likely middle) phalange V and terminal phalanx I of the foot, never develop.

Discussion

The ontogeny of the skeleton in frogs with direct development, and how it diverges from known patterns in
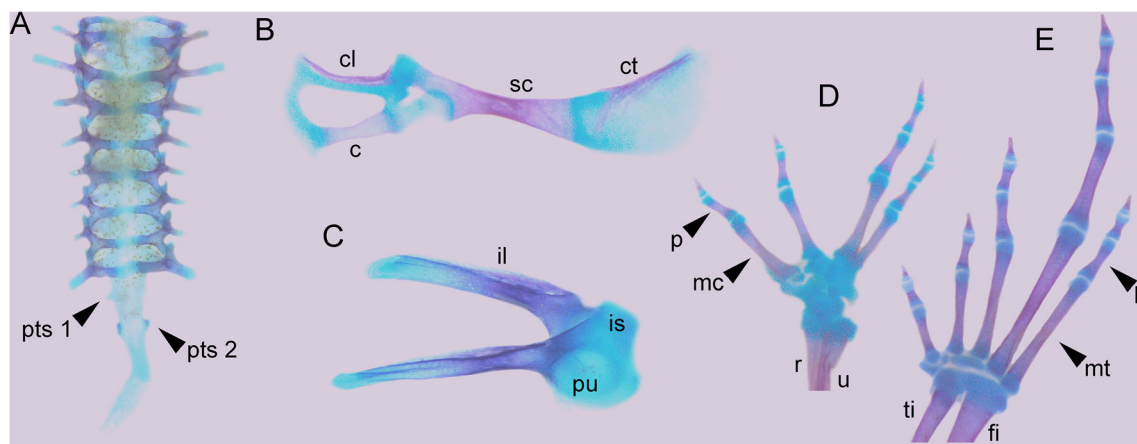

Fig. 8 Postcranial skeleton of *Haddadus binotatus* at TS15. **a** Vertebral column, dorsal view. **b** Pectoral girdle, ventral view. **c** Pelvic girdle, lateral view. **d** Forelimb, dorsal view. **e** Hind limb, dorsal view. *Abbreviations*: *c*, coracoid; *cl*, clavicle; *ct*, cleithrum; *fi*, fibulare; *il*, ilium; *is*, ischium; *mc*, metacarpalia; *mt*, metatarsalia; *p*, phalanges; *pts*, postsacral vertebra; *pu*, pubis; *r*, radius; *sc*, scapula; *ti*, tibiale; *u*, ulna. *Scale bars* = 1 mm

Fig. 9 Schematic representation of auto- and zeugopodium development in *Haddadus binotatus*. **a** Forelimb. **b** Hind limb. The adult configuration is shown at the left, and drawings at the right show the sequential ossification (black segments) of elements. *Abbreviations*: *fi*, fibulare; *mc*, metacarpalia; *mt*, metatarsalia; *p*, phalanges; *ph*, prehallux; *pp*, prepollex; *r*, radius; *ra*, radiale; *ti*, tibiale; *u*, ulna; *ul*, ulnare; *Y*, element Y; *1–5*, distal carpalia and tarsalia; *I–V*, fingers and toes
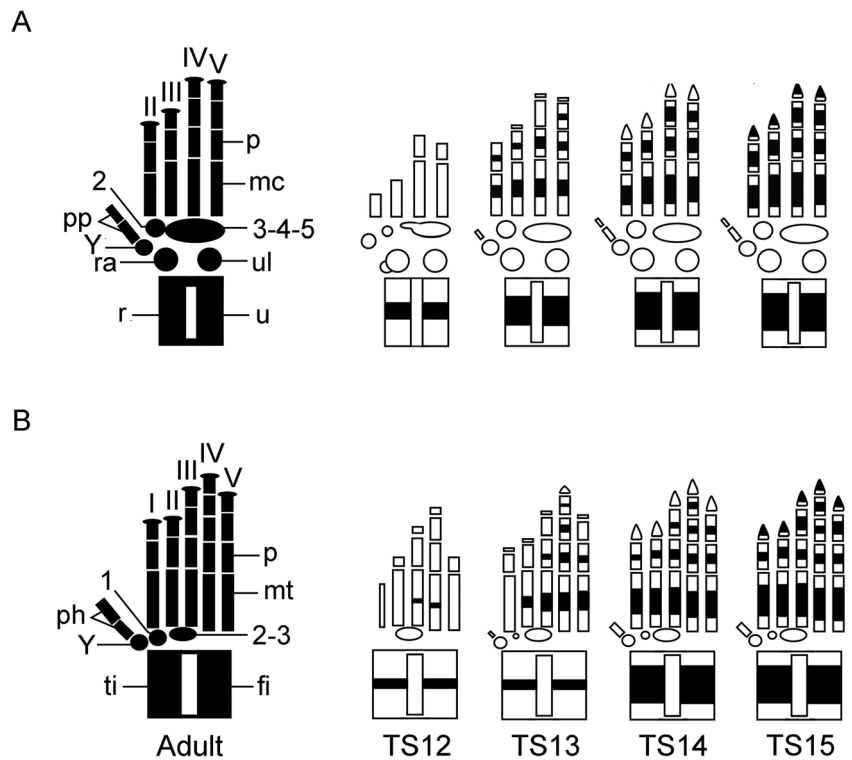
metamorphosing species, has interested biologists for decades. In their detailed study of *E. coqui*, Hanken et al.

(1992) discussed processes involved in shaping the particular skeletal ontogenetic trajectory in this and related species. They
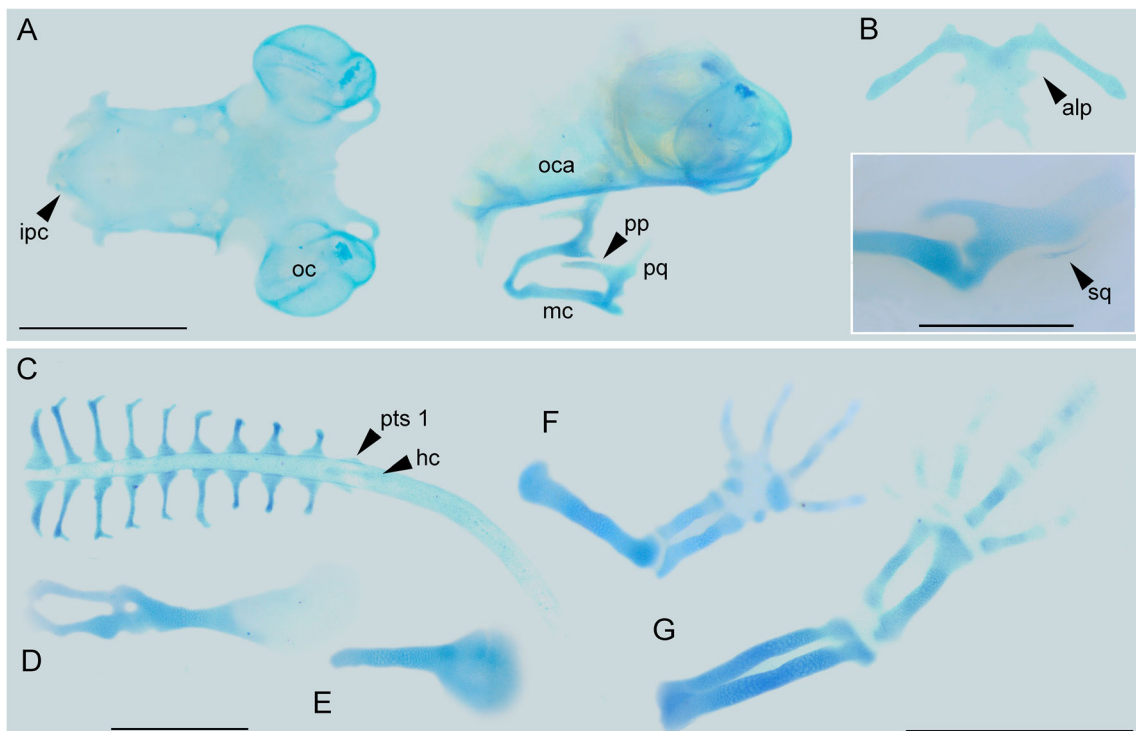

Fig. 10 Skeletal morphology of *Ischnocnema henselii* at TS11–12. **a** Skull dorsal and lateral views. **b** Hyobranchial apparatus, ventral view. *Inset*: detail of the palatoquadrate cartilage, showing a primordium of the squamosal. **c** Vertebral column, dorsal view. **d** Pectoral girdle, ventral view. **e** Pelvic girdle, lateral view. **f** Forelimb, dorsal view. **g** Hind limb, dorsal view. *Abbreviations*: *alp*, anterolateral process; *hc*, hypochord; *ipc*, inferior prenasal cartilage; *mc*, Meckel's cartilage; *oc*, otic capsule; *oca*, orbital cartilage; *pp*, pterygoid process; *pq*, palatoquadrate; *pts*, postsacral vertebra; *sq*, squamosal. *Scale bars* = 1 mm

Fig. 11 Cranial skeleton of *Ischnocnema henselii* at hatching. Dorsal, ventral, lateral, and frontal views. *Abbreviations*: *as*, angulosplenial; *d*, dentary; *eo*, exoccipital; *fp*, frontoparietal; *m*, maxilla; *n*, nasal; *np*, neopalatine; *pm*, premaxilla; *po*, prootic; *ps*, parasphenoid; *pt*, pterygoid; *qj*, quadratojugal; *sm*, septomaxilla; *sq*, squamosal; *v*, vomer. *Scale bar* = 1 mm
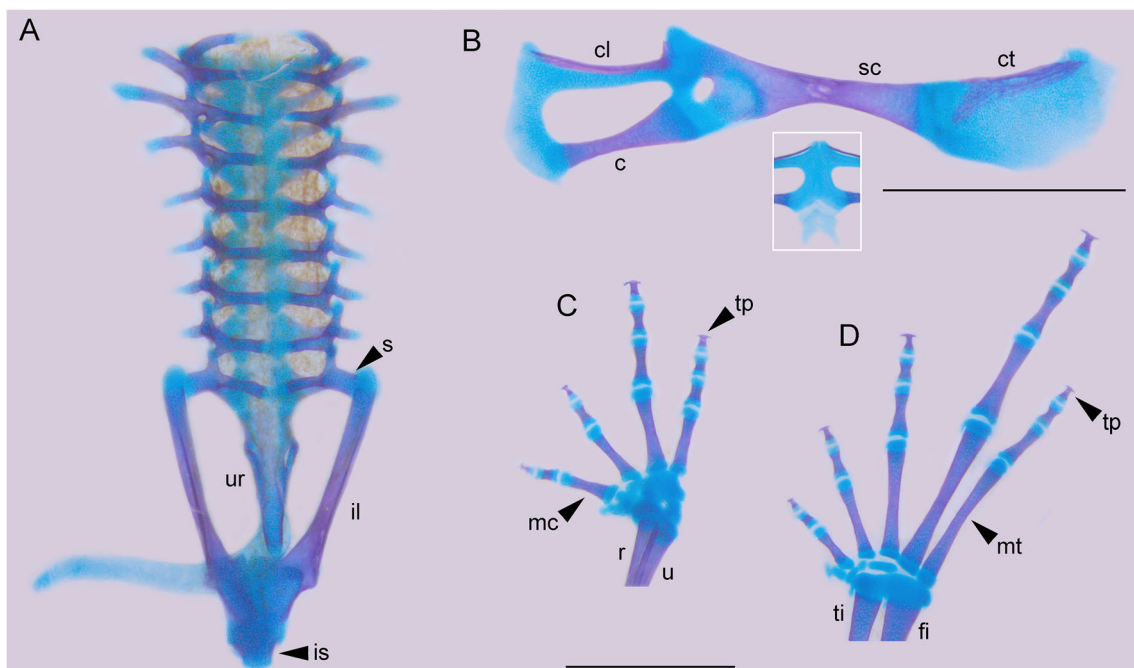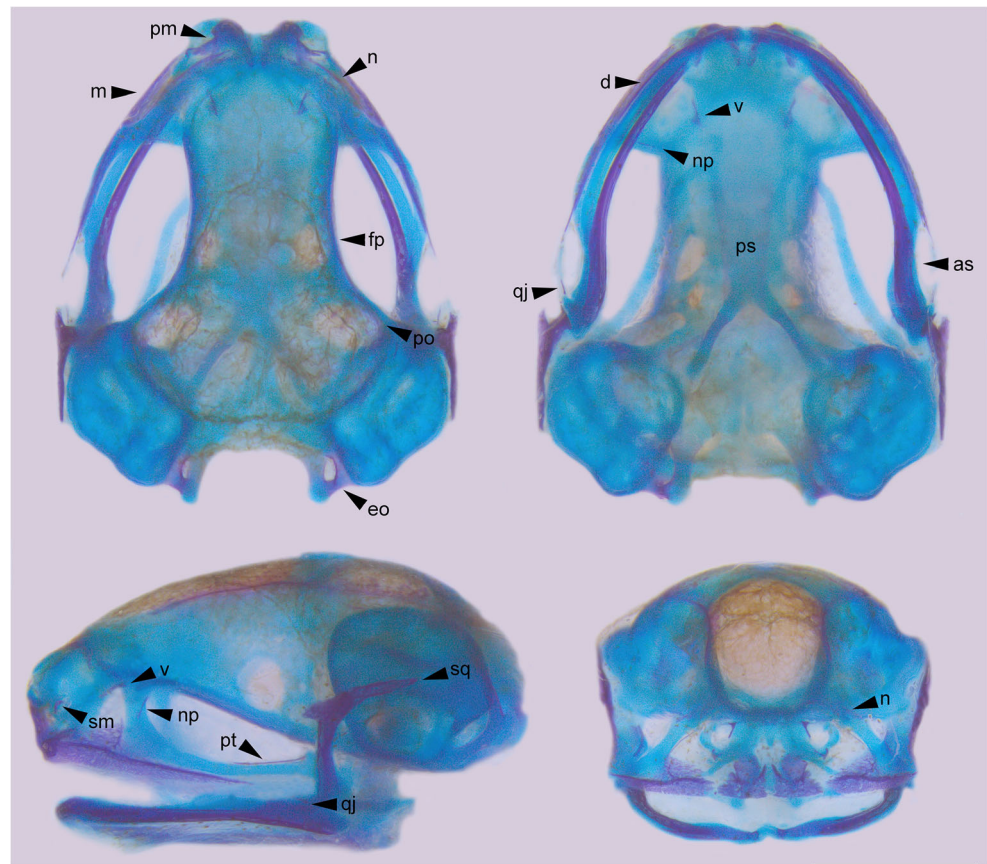
Fig. 12 Postcranial skeleton of *Ischnocnema henselii* at hatching. **a** Vertebral column and pelvic girdle, dorsal view. **b** Pectoral girdle, ventral view. **c** Forelimb, dorsal view. **d** Hind limb, dorsal view. The inset shows detail of the medial region of articulated pectoral girdle, with a developing bifurcate xiphisternum. *Abbreviations*: *c*, coracoid; *cl*, clavicle; *ct*, cleithrum; *fi*, fibulare; *il*, ilium; *is*, ischium; *mc*, metacarpalia; *mt*, metatarsalia; *r*, radius; *s*, sacrum; *sc*, scapula; *ti*, tibiale; *tp*, T-shaped phalanges; *u*, ulna; *ur*, urostyle. *Scale bars* = 1 mm
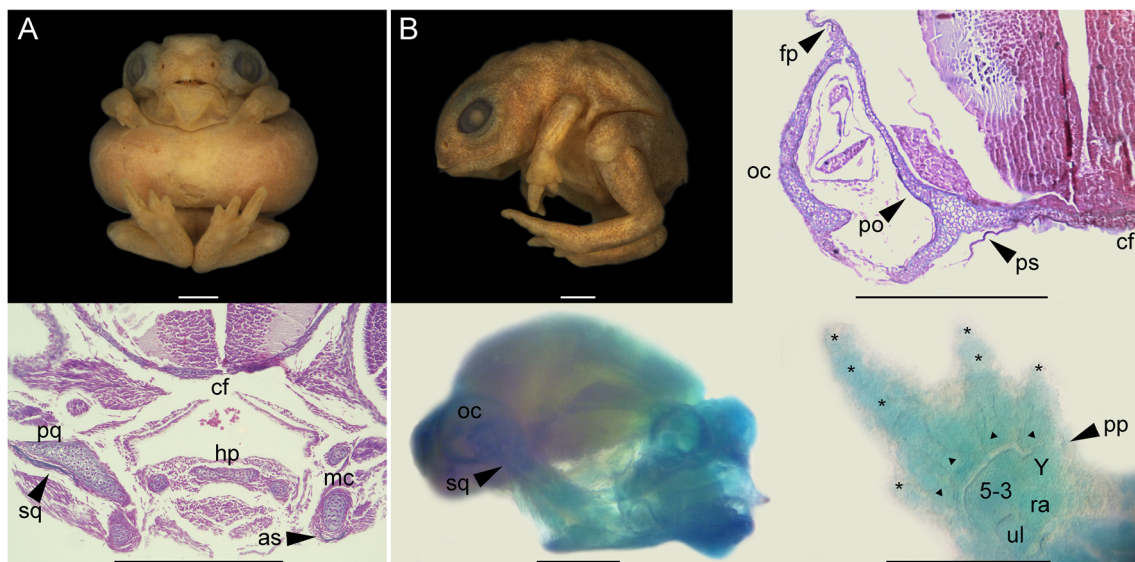
Fig. 13 Cranial and postcranial skeleton of *Brachycephalus ephippium* at late prehatching stages. **a** Embryo at TS13, showing a cross section of the lower jaw with ossified squamosals and angulosplenials investing the palatoquadrate and Meckel's cartilage. **b** Embryo at TS15, showing a cross section through the otic capsule, showing the still slight ossification, and cleared and stained chondrocranium (anterolateral view) and left hand (dorsal view). Histological sections are colored with Masson's trichrome stain. *Abbreviations*: *cf*, angulosplenial; *cf*, cranial floor; *fp*, frontoparietal; *hp*, hyoid plate; *mc*, Meckel's cartilage; *oc*, otic capsule; *po*, prootic; *pp*, prepollex; *pq*, palatoquadrate; *ps*, parasphenoid, *ra*, radiale; *sq*, squamosal; *ul*, ulnare; *Y*, element Y likely plus carpale 2; *5–3*, distal carpalia 3–5. Small triangles in the hand indicate metacarpalia II–V, and asterisks the finger phalanges. *Scale bars* = 0.5 mm

reported a combination of partial recapitulation of the ancestral biphasic development plus a fundamental repatterning that includes loss and appearance of structures and heterochronic shifts in developmental events. These processes concern both the cartilaginous scaffolds of cranial and postcranial regions and the structure and sequence of differentiation of osseous elements.

Skull developmental patterns in Brachycephaloidea

Chondrocranial development is in general similar among the species examined here and in comparison to *E. coqui* (Hanken et al. 1992). All these taxa show a conspicuous remodeling of the ethmoidal and suspensorial regions, with main changes involving the absence of some typically larval cartilages and a mid-metamorphic shape at first appearance in others. Suprarostral cartilages, trabecular horns, three palatoquadrate processes (muscular, larval otic, and ascending processes), and quadratocranial commissures never develop. In turn, the pterygoid processes, which form the adult connection between suspensorium and neurocranium, develop very early. In *E. coqui*, Kerney et al. (2010) found suprarostral anlagen in the frontonasal region and suggested that the loss of these cartilages could be due to a change in the timing of chondrocyte differentiation. Conversely, these authors stress that the absence of a quadratocranial commissure likely implies a developmental repatterning leading to differentiation of the adult bridge to the neurocranium without a preceding larval connection. In addition, the nasal cartilages of all brachycephaloid

species studied differentiate with an adult-like configuration, and before hatching, they already exhibit their definitive appearance. Similarly, the lower jaw differentiates with the inverted U-shape typical of metamorphic stages of biphasic anurans. Heterochronic shifts are evident among these taxa. Chondrocranial ontogeny appears to be overall faster in *I. henselii* and slower in *O. barituensis* (Table 2), whereas *H. binotatus* combines an accelerated chondrogenesis of cranial elements with a delayed development of the hyoid apparatus. The two specimens of *B. ephippium* show the most delayed chondrocranial development: almost at hatching, the palatoquadrate still does not reach its adult arrangement and the rostrum is very short.

Skull development in Brachycephaloidea is known in detail for *E. coqui*, and some more limited information is available for *Eleutherodactylus nubicola* (Lynn 1942), *Eleutherodactylus ricordii* (Hughes 1959), and *Ischnocnema guentheri* (Lynn and Lutz 1946). Patterns in these species differ in two main aspects regarding those with biphasic ontogeny (Hanken et al. 1992). First, bone formation is predisplaced into the embryonic period, with only a few elements ossifying after hatching. In *E. coqui*, 14 of the total 18 adult bones ossify before or shortly after hatching, whereas vomers, neopalatines, sphenethmoid, and hyoid posterior processes ossify at some point during posthatching life (Table 4). Embryos of *H. binotatus* and *Ischnocnema* show an even more accelerated ossification, and 17 bones out of 18 are distinct as early as 0–4 days after hatching. Conversely, embryos of *O. barituensis* exhibit an overall slower ossification

rate, with the said bones plus the mentomeckelians and quadratojugals remaining undifferentiated at hatching. In *B. ephippium*, the limited data indicate that ossification rate in prehatching stages is lower, and at TS15, several jaw and nasal bones are apparently not differentiated yet. Interestingly, nothing of the hyperossification and extensive bone fusion that characterizes this species can be foreseen at these early stages. The juvenile specimens studied (about twice as large as the embryos we describe) do show most cranial elements well ossified, but parotic plates are still nonornamented and independent from frontoparietals and squamosals (Campos et al. 2010).

Second, the timing of differentiation of each cranial element relative to other parts also changes in direct-developing brachycephaloids relative to metamorphosing species. Weisbecker and Mitgutsch (2010) synthesized information about skull developmental patterns in anurans and revealed that ossification sequences tend to be highly conserved at the beginning and the end, while those bones ossifying at middle stages are the most interspecifically variable. The ossification pattern in biphasic-developing anurans commonly starts with the ossification of braincase bones, typically the exoccipitals, frontoparietals, and the parasphenoid (Trueb 1985). The main shift in brachycephaloids consists of a precocious ossification of jaw and suspensorium bones, always preceding the ossification of braincase and otic elements. In addition, some species-specific variations change the ossification sequence of individual bones (Table 4). Angulosplenials and squamosals are the first to ossify in all known brachycephaloids. They are followed in general by premaxillae, maxillae, dentaries, and pterygoids, and in the braincase, parasphenoid and frontoparietals. The exoccipitals ossify along with most of the former elements in *E. coqui*, *H. binotatus*, and *I. henselii*, but later in *O. barituensis*. The mentomeckelians, quadratojugals, and septomaxillae ossify next in most species. However, the mentomeckelians of *Ischnocnema* and the quadratojugals of *Haddadus* appear earlier, whereas both elements appear much later in *Oreobates*. Finally, nasals and prootics are in general the last bones to ossify before hatching. In *E. nubicola*, however, these and the septomaxillae ossify after hatching (Lynn 1942). Ossification timing of the four remaining bones of the brachycephaloid adult cranial plan are variable. The vomers and hyoid posterior processes ossify after hatching in *E. coqui* and *Oreobates* but before in *Haddadus* and *Ischnocnema*, and the neopalatines are evident in newly hatched specimens of *Haddadus* and *Ischnocnema*. As in the vast majority of anuran species, the sphenethmoid is the last bone to differentiate in all brachycephaloids examined so far.

The development of the osteocranium has been investigated in a few other endotrophic amphibian species, including anuran clades, caecilians, and salamanders. The precocious differentiation of jaw and suspensorium bones emerges as a pattern shared by several taxa. Hanken et al. (1992) commented on the similar ossification sequences of *Eleutherodactylus* species, paraviviparous *Pipa pipa*, and the viviparous caecilian *Dermophis mexicanum.* Nidicolous tadpoles of *Eupsophus* also show early ossification of the squamosals and upper and lower jaws (Vera Candioti et al. 2005, 2011). Likewise, obligate and partially endotrophic species of hynobiid salamanders show a similarly altered ossification sequence as compared with congeneric taxa (Vassilieva et al. 2015). Functional explanations related to early feeding have been invoked to account for these heterochronic changes (Wake and Hanken 1982; Hanken et al. 1992; Yeh 2002a; Weisbecker and Mitgutsch 2010). However, further knowledge of the diversity of osteogenesis within and outside these groups challenges some interpretations, especially by raising questions about the plesiomorphic states and thus the unequivocal relationship with developmental modes. For instance, Yeh (2002a) discussed the shifts in the timing of jaw ossification in pipoids, highlighting that the pronounced acceleration in *Pipa pipa* evolved within a group with an already early jaw ossification. The author interprets that this acceleration is possible due to the reduction of larval jaw cartilages that characterizes all pipoids irrespective of their developmental mode. In rhacophorids, Kerney et al. (2007) and Vassilieva (2017) integrated information on species with and without free-living larval stages. Comparative analysis shows that direct developers share the initial differentiation of two braincase bones with metamorphic species, but differ in the degree of acceleration of jaw and suspensorium ossification. In caecilians, Müller and collaborators discussed available data on ossification sequences in viviparous, direct-developing, and free-living larva species (Müller et al. 2005; Müller 2006; Theska et al. 2019). They found differences between viviparous and direct developers that, as suggested by Wake and Hanken (1982), could be related to intrauterine feeding, but failed to achieve robust conclusions given the currently insufficient information about the whole group.

Postcranial ontogeny in Brachycephaloidea

Information about postcranial development in direct-developing species is even more scant than for cranial ontogeny, and complete ossification data are available only for the axial skeleton. Comparative analyses including the four additional brachycephaloids in this study show that morphogenesis of the axial and appendicular skeleton is highly conserved, with main variations including the extent of ossification at hatching and those aspects related to diagnostic features of *Brachycephalus*.

To our knowledge, descriptions concerning development of the axial skeleton in direct-developing frogs are restricted to *E. coqui*, *E. johnstonei*, and *Craugastor raniformis* (Hanken et al. 1992; Meza-Joya et al. 2013). The species we examined

follow the same overall pattern of chondrification and ossification (Table 4). Events occur at comparable stages, and vertebrae differentiate and ossify in a cephalocaudal direction, with a delayed onset of ossification of centra relative to the neural arches. This feature has been highlighted as one of the main differences regarding metamorphosing species (Meza-Joya et al. 2013). Among the studied direct developers, the most variable aspect lies in the ontogeny of the postsacral region and its configuration at hatching. As in several metamorphosing species (e.g., Púgener and Maglia 2009), the ossification of the hypochord occurs separately from that of other components of the urostyle. The hypochord ossifies earlier than the coccyx in H. binotatus, and later in O. barituensis. At hatching, O. barituensis and H. binotatus show postsacral elements still discrete; conversely, I. henselii has an almost fully formed urostyle. Finally, there is no evidence of the distinct paravertebral plates of B. ephippium at hatching; they acquire adult configuration later during posthatching stages (Campos et al. 2010).

The sequence of chondrification and ossification in pectoral and pelvic girdles proceeds in a similar manner in species analyzed here (Table 4). The onset in the ossification of both girdles is simultaneous with the ossification of the proximal parts of limbs. As in other skeletal regions, ossification in I. henselii is apparently faster than in H. binotatus, and O. barituensis shows the most delayed sequence. In the pectoral girdle, the ossification sequence is conserved, with the scapulae being the first elements to ossify, followed by the clavicles, coracoids, cleithra, and finally some areas of the suprascapulae. This is similar to what has been described for several terrestrial metamorphosing species, in contrast to some aquatic or semi-aquatic forms in which the ossification of the scapula is significantly delayed (e.g., Haas 1999; Soliz et al. 2018). At hatching, most portions of the pectoral girdle of all examined species remain cartilaginous. Elements of the sternum develop after hatching in all species but I. henselii, where slightly chondrified meso- and xiphisterna are present in the recently hatched specimen. The complete ossification of the epicoracoids, coracoids, and clavicles, autapomorphic of Brachycephalus (e.g., Pombal Jr and Gasparini 2006), is likely acquired late during posthatching life. In turn, ossification of the pelvic girdle begins from TS12 in all species examined, with endochondral ossification of the ilia. At hatching, the ischia of the four examined species are slightly ossified. The iliosacral articulation seems to be defined at TS13–14, with the iliac shafts parallel to the vertebral column and reaching the level of the sacral diaphyses. In metamorphic taxa, this coincides with the complete loss of the vent tube, before the beginning of the events of tail resorption (e.g., Fabrezi and Goldberg 2009).

Limb development is usually regarded as a well-known example of heterochronic change during the evolution of direct development in anurans, since its onset takes place during neurulation, early in the embryonic period instead of during larval stages as in biphasic cycle frogs (Townsend and Stewart 1985; Richardson et al. 1998). Hanken et al. (2001) and later Kerney and Hanken (2008) described limb development in E. coqui and found highly conserved patterns in skeletal condensations combined with developmental novelties. Regardless of the overall acceleration, the morphogenesis of primary cartilages follows the proximodistal and posteroanterior sequences of differentiation typical of metamorphosing frogs and almost all other tetrapods (e.g., Shubin and Alberch 1986; Fabrezi and Goldberg 2009). However, the initial patterning of limb development (e.g., as revealed by the early expression of distal skeletal precursors) departs from the prevailing models of vertebrate limb formation (see also Gross et al. 2011).

In the species we examined, although developmental series are not complete enough to trace early limb chondrogenesis, we can elucidate some patterns (Table 3). In general, limb development in O. barituensis and at least some events concerning differentiation of distal elements of H. binotatus seem to be slightly delayed as compared with those of E. coqui, both in stages and developmental time (time data in Townsend and Stewart 1985; Goldberg et al. 2012; Goldberg and Vera Candioti 2015). In contrast, the distalmost elements of digits of fore- and hind limbs of I. henselii develop comparatively early. As in E. coqui, limb development is slightly asynchronous in O. barituensis and likely in the three remaining species. Hind limb chondrification begins earlier and progresses somehow faster than forelimb chondrification, despite the fact that hind and forelimb buds appear simultaneously in O. barituensis or hind limb differentiation is slightly predisplaced in H. binotatus (Goldberg et al. 2012; Goldberg and Vera Candioti 2015).

The anuran carpus is formed by the ulnare, radiale, element Y, four distal carpals, and prepollical elements (Fabrezi et al. 2017). In the brachycephaloid species we examined, these elements result from different ontogenetic pathways. The ulnare may arise as a single element (H. binotatus) or from the fusion of the condensation of the ulnare plus an embryonic condensation of the intermedium (O. barituensis). In turn, the radiale involves two different cartilaginous primordia that fuse later, a condition already described in several leptodactylids and hylids (Fabrezi and Barg 2001). Fabrezi and Alberch (1996) interpreted the anterior condensation as the radiale itself; the identification of the second element remains problematic since it could represent a de novo condensation or derive from different preaxial cartilages, which would imply an until now unknown ramification in the preaxial series (Shubin and Alberch 1986). The element Y arises from one (H. binotatus) or two (O. barituensis) cartilaginous elements. Despite their different ontogenetic pathways, these proximal carpal elements end up in single structures that remain independent in adult specimens of Haddadus, Ischnocnema, and Oreobates. Likewise, disregarding slight differences in distal carpal

differentiation, the adult configuration in these three taxa includes distal carpalia 3–5 fused, and a small, independent distal carpale 2. The ontogeny of prepollical elements is slightly variable, with a delayed differentiation of the distal element in *O. barituensis*. Species of *Eleutherodactylus* show this same carpal morphology, with six independent elements (e.g., Guayasamin 2004). On the other hand, the identity and arrangement of carpal bones in *Brachycephalus* has not yet been discussed in depth. The most generalized pattern is described as consisting of distal carpalia 2–5 and element Y fused and prepollex absent or present as a single element (e.g., Ribeiro et al. 2017). Three species differ by having two prepollical elements (*Brachycephalus actaeus* and *B. ephippium*), or an independent element Y (*Brachycephalus darkside* and *B. ephippium*) (Guimarães et al. 2017; Monteiro et al. 2018; Morphosource n.d.). However, developmental patterns of the anuran carpus known to date do not include fusion of distal carpale 2 with the remaining distal carpals but with element Y (Fabrezi et al. 2017). Thus, the independent element in these two latter species most like represents an element Y + c2, making the largest bone the fused c3–5.

In turn, the anuran tarsus is formed by the tibiale, fibulare, element Y, up to three distal tarsals, and prehalluxical elements (Fabrezi et al. 2017). Unlike in hands, tarsal elements in brachycephaloid species follow a rather conserved ontogenetic trajectory that ends in fused and enlarged tibiale–fibulare, distal tarsale 1, distal tarsale 2–3, element Y, and two prehalluxical elements in the adult. The only variation is in element Y, which can arise as a single element (*H. binotatus*) or as two, dorsal and ventral, condensations that later fuse (*O. barituensis*). Carpal and tarsal sesamoids described in adult specimens of brachycephaloids analyzed are not developed in prehatching stages.

In *Oreobates* and *Haddadus*, limb development reveals an invariant sequence of digit formation, IV–V–III–II for fingers and IV–III–V–II–I for toes, with digit V included in the digital arch as in almost all tetrapods (Fabrezi et al. 2017). Conversely, in *Brachycephalus*, the differentiation of finger III and toe II precedes that of the reduced phalanx of digits V, and the last digits to differentiate are then the two outermost. Changes in the number of digits have been shown to likely occur through an ordered evolutionary sequence (Alberch and Gale 1985; Shubin and Alberch 1986). In this sense, the loss of terminal phalanges in finger II and toe I in *Brachycephalus* species is still consistent with proposed models of autopodium development, which state that first digits are usually the last to start chondrification and then are likely to be lost by development truncation (Alberch and Gale 1985; Hanken 1993; Yeh 2002b). Deviations from the expected pattern of loss of autopodium elements occur in unrelated amphibians, and they are suggested to be explained by a respecification of the number and spatial organization of skeletal elements caused by a reduction in limb absolute size (Alberch and Gale 1985).

Ossification begins almost simultaneously in fore- and hind limbs (Table 4), and the sequence of ossification of elements matches closely the chondrogenetic pattern, as it occurs in species with biphasic development (e.g., Fabrezi and Goldberg 2009; Fabrezi et al. 2017). A noteworthy difference regarding metamorphosing species (e.g., Wiens 1989; Perotti 2001; Fabrezi and Goldberg 2009) is that ossification of the autopodium in direct-developing species we examined begins well before all terminal phalanges are formed. Interspecific differences include a slightly accelerated ossification in *H. binotatus*, which reaches hatching with limbs more ossified than *O. barituensis*. Interestingly, in these two latter species, the transverse outgrowths that give the terminal phalanges their distinct T-shapes differentiate and ossify after hatching. In contrast, hatched *I. henselii* shows well-ossified T-shaped phalanges in fingers and toes. In comparison, hatched specimens of *E. coqui* apparently show all elements of hind limbs ossified, except for the distal tarsals, and like in *Oreobates* and *Haddadus*, T-shaped terminal phalanges are not present at this stage (Hanken et al. 2001).

A word on integration between cranial and postcranial ontogeny in direct development

All studies about direct development highlight the "mosaic" nature of this developmental mode, which combines several pathways conserved from ancestral biphasic ontogenies with novel features involving structural and heterochronic shifts (e.g., Hanken et al. 2001). These include the codissociation of characters, defined as changes in developmental timing of some suites of characters relative to other characters. Schlosser (2001, 2008) summarized patterns of temporal shifts in the development of limbs, nervous system, and pharyngeal arches in *E. coqui* and highlighted that the initial precocious development of limbs is later reverted by a predisplaced metamorphic remodeling of cranial structures. In addition, Ziermann and Diogo (2013) stated that the cryptic metamorphosis that direct developers undergo involves a decoupling of muscular versus cartilage development in the hyoid and branchial regions. Patterns of ossification of cranial and postcranial regions in the brachycephaloid species we examined indicate that the onset of differentiation of bony elements is precocious in the postcranium, and this renders free-living hatchlings with more robust axial and appendicular systems. Patterns of ossification of cranium versus postcranium are not thoroughly explored across anurans, but some specific studies emphasize on some differences related to life history aspects (e.g., Senevirathne et al. 2016).

Interspecific variations in timing and sequence of chondrification and ossification of cranium and postcranium need to be further explored in Brachycephaloidea, considering also possible interpopulational diversity. The skeletal development mostly delayed in *Oreobates* and mostly accelerated

in *Ischnocnema* relative to *Haddadus* and *E. coqui* is apparently not related to size or time at hatching. Hatchling length is similar in most known brachycephaloids (about 6 mm; except for *H. binotatus*, which are larger), and prehatching development lasts 20–35 days in all these taxa (reviewed in Goldberg et al. 2020). In turn, some skeletal features of *B. ephippium* can be discussed as paedomorphic characters associated with miniaturization. The overall delayed chondro- and osteocranial development that we observe may explain in part the pattern of anteriorized jaw articulation discussed by Yeh (2002b) in several groups of small frogs. The loss of some cranial and autopodial bones has been consistently related to a significant decrease in body size (Alberch and Gale 1985; Yeh 2002b). Likewise, the adult independent element Y + carpale 2 of the hands of *B. ephippium* could represent the retention of the carpal morphology of early stages of related species. Conversely, a prepollex composed of two elements (occurring only in *B. ephippium* and *B. actaeus*) retains the morphology likely ancestral for brachycephaloids. The diversity of carpal anatomy likely adds one further element to the description by Trueb and Alberch (1985) of this species as a "morphological contradiction" that combines several paedomorphic features with an outstanding peramorphic hyperossification. It is interesting to note that, other than in *Brachycephalus* where it has been discussed as related to miniaturization, no brachycephaloid nor direct developer from different anuran families has been reported to undergo reduction or loss of bones, as it occurs in endotrophic salamanders (Vassilieva et al. 2015). This could be related to the fact that salamanders develop transient skull bones (coronoid and palatine) that do not survive metamorphosis and are the last to ossify.

Final remarks

Direct development evolved numerous times during amphibian phylogeny (e.g., Schweiger et al. 2017), and in this context, it is reasonable to expect different sets of clade-specific features. This is already reported in several character systems exhibiting high variation in the presence, morphology, and developmental timing across anuran groups, such as gas-exchange structures (e.g., gills, opercules, tails, abdominal sacs), hatching structures (egg tooth, hatching cells), adhesive glands, vent tube, and limbs (e.g., Hanken et al. 1992; Bahir et al. 2005; Anstis et al. 2007; Narayan et al. 2011; Goldberg and Vera Candioti 2015; Schweiger et al. 2017). Skeletal ontogeny seems to follow the same pattern, with heterochronic shifts likely different among groups. Along with the egg tooth and the enveloping tail with transverse fins, apomorphic at different levels in Brachycephaloidea (e.g., Goldberg et al. 2020), an ossification sequence with extremely accelerated ossification of jaws and suspensorium could be distinctive of the clade. In addition, the genus *Eleutherodactylus* has long

been regarded as extreme among anurans with respect to the degree to which its development deviates from the ancestral biphasic ontogeny (e.g., Lynn 1961; Schlosser 2008). Our results highlight that the large brachycephaloid clade, with Eleutherodactylidae recovered as a basal family (Padial et al. 2014), exhibits a wide morphological diversity that appears to be even more derived instead, regarding several external characters (gills, tail, vent tube) as well as a skeletal developmental patterns.

References

Alberch, P., & Gale, E. (1985). A developmental analysis of an evolutionary trend: digital reduction in amphibians. *Evolution, 39*, 8–23.

Anstis, M., Roberts, J. D., & Altig, R. (2007). Direct development in two myobatrachid frogs, *Arenophryne rotunda* Tyler and *Myobatrachus gouldii* Gray, from Western Australia. *Records of the Western Australian Museum, 23*, 259–271.

Bahir, M. M., Meegaskumbura, M., Manamendra-Arachchi, K., Schneider, C. J., & Pethiyagoda, R. (2005). Reproduction and terrestrial direct development in Sri Lankan shrub frogs (Ranidae: Rhacophorinae: *Philautus*). *The Raffles Bulletin of Zoology, 12*, 339–350.

Campos, L. A., Da Silva, H. R., & Sebben, A. (2010). Morphology and development of additional bony elements in the genus *Brachycephalus* (Anura: Brachycephalidae). *Biological Journal of the Linnean Society, 99*, 752–767.

Cocteau, T. (1835). Sur un genre peu connu et imparfaitement décrit de batraciens anoures à carapace dorsale osseuse, et sur une nouvelle espèce de ce genre. *Magasin de Zoologie, d'Anatomie Comparée et de Palaeontologie, Guérin, 5*, 20–31 and Pl. 7–8.

de Lima, A. V. P., Reis, A. H., Amado, N. G., Cassiano-Lima, D., Borges-Nojosa, D. M., Oriá, R. B., & Abreu, J. G. (2016). Developmental aspects of the direct-developing frog *Adelophryne maranguapensis*. *Genesis, 54*, 257–271.

Fabrezi, M., & Alberch, P. (1996). The carpal elements of anurans. *Herpetologica, 52*, 188–204.

Fabrezi, M., & Barg, M. (2001). Patterns of carpal development among anuran amphibians. *Journal of Morphology, 249*, 210–220.

Fabrezi, M., & Goldberg, J. (2009). Heterochrony during skeletal development of *Pseudis platensis* (Anura, Hylidae) and the early offset of skeleton development and growth. *Journal of Morphology, 270*, 205–220.

Fabrezi, M., Goldberg, J., & Chuliver Pereyra, M. (2017). Morphological variation in anuran limbs: constraints and novelties. *Journal of Experimental Zoology Part B, 328*, 546–574.

Goldberg, J., & Vera Candioti, F. (2015). A tale of a tail: variation during the early ontogeny of *Haddadus binotatus* (Brachycephaloidea: Craugastoridae) as compared with other direct developers. *Journal of Herpetology, 49*, 479–484.

Goldberg, J., Vera Candioti, F., & Akmentins, M. S. (2012). Direct developing frogs: ontogeny of *Oreobates barituensis* (Anura: Terrarana) and the development of a novel trait. *Amphibia-Reptilia, 33*, 239–250.

Goldberg, J., Taucce, P. P. G., Quinzio, S., Haddad, C. F. B., & Vera Candioti, F. (2020). Increasing our knowledge on direct-developing frogs: ontogeny of *Ischnocnema henselii* (Anura: Brachycephalidae). *Zoologischer Anzeiger, 284*, 78–87.

Goutte, S., Mason, M. J., Antoniazzi, M. M., Jared, C., Merle, D., Cazes, L., Toledo, L. F., Hafci, H., Pallu, S., Portier, H., Schramm, S., Gueriau, P., & Thoury, M. (2019). Intense bone fluorescence reveals hidden patterns in pumpkin toadlets. *Scientific Reports, 9*, 5388.

Gross, J. B., Kerney, R., Hanken, J., & Tabin, C. J. (2011). Molecular anatomy of the developing limb in the coqui frog, *Eleutherodactylus coqui*. *Evolution & Development, 13*, 415–426.

Guayasamin, J. M. (2004). The *Eleutherodactylus orcesi* species group (Anura: Leptodactylidae): comparative osteology and comments on its monophyly. *Herpetological Monographs, 18*, 142–174.

Guimarães, C. S., Luz, S., Carvalho Rocha, P., & Neves Feio, R. (2017). The dark side of pumpkin toadlet: a new species of *Brachycephalus* (Anura: Brachycephalidae) from Serra do Brigadeiro, southeastern Brazil. *Zootaxa, 4258*, 327–344.

Haas, A. (1999). Larval and metamorphic skeletal development in the fast-developing frog *Pyxicephalus adspersus* (Anura, Ranidae). *Zoomorphology, 119*, 23–35.

Haddad, C. F. B., & Prado, C. (2005). Reproductive modes in frogs and their unexpected diversity in the Atlantic Forest of Brazil. *BioScience, 55*, 207–2017.

Hanken, J. (1993). Adaptation of bone growth to miniaturization of body size. In Hall, B. K. (Ed.), *Bone. Vol. 7. Bone growth* (pp. 79–104). Boca Ratón: CRC Press.

Hanken, J., Klymkowsky, M. W., Summers, C. H., Seufert, D. W., & Ingebrigtsen, N. (1992). Cranial ontogeny in the direct-developing frog, *Eleutherodactylus coqui* (Anura: Leptodactylidae), analyzed using whole-mount immunohistochemistry. *Journal of Morphology, 211*, 95–118.

Hanken, J., Carl, T. F., Richardson, M. K., Olsson, L., Schlosser, G., Osabutey, C. K., & Klymkowsky, M. W. (2001). Limb development in a "nonmodel" vertebrate, the direct developing frog *Eleutherodactylus coqui*. *Journal of Experimental Zoology Part B, 291*, 375–388.

Hughes, A. (1959). Studies in embryonic and larval development in Amphibia. I. The embryology of *Eleutherodactylus ricordii*, with special reference to the spinal cord. *Journal of Embryology and Experimental Morphology, 7*, 22–38.

Kerney, R., & Hanken, J. (2008). Gene expression reveals unique skeletal patterning in the limb of the direct-developing frog, *Eleutherodactylus coqui*. *Evolution & Development, 10*, 439–448.

Kerney, R., Meegaskumbura, M., Manamendra-Arachchi, K., & Hanken, J. (2007). Cranial ontogeny in *Philautus silus* (Anura: Ranidae: Rhacophorinae) reveals few similarities with other direct-developing anurans. *Journal of Morphology, 268*, 715–725.

Kerney, R., Gross, J. B., & Hanken, J. (2010). Early cranial patterning in the direct-developing frog *Eleutherodactylus coqui* revealed through gene expression. *Evolution & Development, 12*, 373–382.

Lynn, W. G. (1942). The embryology of *Eleutherodactylus nubicola*, an anuran which has no tadpole stage. *Contributions to Embryology, 541*, 27–62.

Lynn, W. G. (1961). Types of amphibian metamorphosis. *American Zoologist, 1*, 151–161.

Lynn, W. G., & Lutz, B. (1946). The development of *Eleutherodactylus guentheri* Stdnr. 1864. *Boletim do Museu Nacional Zoologia (N.S.), 71*, 1–46.

Meza-Joya, F. L., Ramos-Pallares, E. P., & Ramírez-Pinilla, M. P. (2013). Ontogeny of the vertebral column of *Eleutherodactylus johnstonei* (Anura: Eleutherodactylidae) reveals heterochronies relative to metamorphic frogs. *The Anatomical Record, 296*, 1019–1030.

Miranda-Ribeiro, A. (1920). Os brachycephalideos do Museu Paulista (com tres especes novas). *Revista do Museu Paulista, 12*, 307–316.

Monteiro, J. P. D., Condez, T. H., Anchietta Garcia, P. C., Comitti, E. J., Amaral, I. B., & Haddad, C. F. B. (2018). A new species of *Brachycephalus* (Anura, Brachycephalidae) from the coasts of Santa Catarina State, southern Atlantic Forest, Brazil. *Zootaxa, 4407*, 483–505.

Morphosource (n.d.). CT-scanned skeleton available at https://www.morphosource.org. *Brachycephalus ephippium* M9209-12426 UF 72725, doi:https://doi.org/10.17602/M2/M12426.

Müller, H. (2006). Ontogeny of the skull, lower jaw, and hyobranchial skeleton of *Hypogeophis rostratus* (Amphibia: Gymnophiona: Caecilidae) revisited. *Journal of Morphology, 267*, 968–986.

Müller, H., Oommen, O. V., & Bartsch, P. (2005). Skeletal development of the direct developing caecilian *Gegeneophis ramaswamii* Taylor, 1964 (Amphibia: Gymnophiona: Caeciliidae). *Zoomorphology, 124*, 171–188.

Narayan, E. J., Hero, M. J., Christi, K. S., & Morley, C. G. (2011). Early developmental biology of *Platymantis vitiana* including supportive evidence of structural specialization unique to the Ceratobatrachidae. *Journal of Zoology, 284*, 68–75.

Nokhbatolfoghahai, M., Mitchell, N. J., & Downie, J. R. (2010). Surface ciliation and tail structure in direct-developing frog embryos: a comparison between *Myobatrachus gouldii* and *Pristimantis* (=*Eleutherodactylus*) *urichi*. *The Herpetological Journal, 20*, 59–68.

Padial, J. M., Grant, T., & Frost, D. R. (2014). Molecular systematics of terraranas (Anura: Brachycephaloidea) with an assessment of the effects of alignment and optimality criteria. *Zootaxa, 3825*, 1–132.

Perotti, M. G. (2001). Skeletal development of *Leptodactylus chaquensis* (Anura: Leptodactylidae). *Herpetologica, 57*, 318–335.

Pombal Jr., J. P., & Gasparini, J. L. (2006). A new *Brachycephalus* (Anura: Brachycephalidae) from the Atlantic Rainforest of the Espírito Santo, southeastern Brazil. *South American Journal of Herpetology, 1*, 87–93.

Pombal Jr., J. P. (1999). Oviposiçao e desenvolvimento de *Brachycephalus ephippium* (Spix) (Anura, Brachycephalidae). *Revista Brasileira de Zoologia, 16*, 967–976.

Púgener, L. A., & Maglia, A. M. (2009). Developmental evolution of the anuran sacro-urostylic complex. *South American Journal of Herpetology, 4*, 193–209.

Ribeiro, L. F., Blackburn, D. C., Stanley, E. L., Pie, M. R., & Bornschein, M. R. (2017). Two new species of the *Brachycephalus pernix* group (Anura: Brachycephalidae) from the state of Paraná, southern Brazil. *PeerJ, 5*, e3603.

Richardson, M., Carl, T., Hanken, J., Elinson, R., Cope, C., & Bagley, P. (1998). Limb development and evolution: a frog embryo with no apical ectodermal ridge (AER). *Journal of Anatomy, 192*, 379–390.

Schlosser, G. (2001). Using heterochrony plots to detect the dissociated coevolution of characters. *Journal of Experimental Zoology Part B, 291*, 282–304.

Schlosser, G. (2008). Development of the retinotectal system in the direct-developing frog *Eleutherodactylus coqui* in comparison with other anurans. *Frontiers in Zoology, 5*, 9. https://doi.org/10.1186/1742-9994-5-9.

Schweiger, S., Naumann, B., Larson, J. G., Möckel, L., & Müller, H. (2017). Direct development in African squeaker frogs (Anura: Arthroleptidae: *Arthroleptis*) reveals a mosaic of derived and

plesiomorphic characters. *Organisms, Diversity and Evolution, 17,* 693–707.

Senevirathne, G., Thomas, A., Kerney, R., Hanken, J., Biju, S. D., & Meegaskumbura, M. (2016). From clinging to digging: the postembryonic skeletal ontogeny of the Indian purple frog, *Nasikabatrachus sahyadrensis* (Anura: Nasikabatrachidae). *PLoS One, 11,* e0151114.

Shubin, N. H., & Alberch, P. (1986). A morphogenetic approach to the origin and basic organization of the tetrapod limb. In M. K. Hecht, B. Wallace, & G. G. Prance (Eds.), *Evolutionary biology* (pp. 319–387). New York: Plenum.

Soliz, M., Ponssa, M. L., & Abdala, V. (2018). Comparative anatomy and development of pectoral and pelvic girdles in hylid anurans. *Journal of Morphology, 279,* 904–924.

Theska, T., Wilkinson, M., Gower, D. J., & Müller, H. (2019). Musculoskeletal development of the Central African caecilian *Idiocranium russeli* (Amphibia: Gymnophiona: Indotyphlidae) and its bearing on the re-evolution of larvae in caecilian amphibians. *Zoomorphology, 138,* 137–158.

Thibaudeau, G., & Altig, R. (1999). Endotrophic anurans, development and evolution. In R. W. McDiarmid & R. Altig (Eds.), *Tadpoles. The biology of anuran larvae* (pp. 170–188). Chicago: University of Chicago Press.

Townsend, D. S., & Stewart, M. M. (1985). Direct development in *Eleutherodactylus coqui* (Anura: Leptodactylidae): a staging table. *Copeia, 1985,* 423–436.

Trueb, L. (1985). A summary of osteocranial development in anurans with notes on the sequence of cranial ossification in *Rhinophrynus dorsalis* (Anura: Pipoidea: Rhinophrynidae). *South African Journal of Science, 81,* 181–185.

Trueb, L., & Alberch, P. (1985). Miniaturization and the anuran skull: a case study of heterochrony. In H. R. Duncker & G. Fleischer G. (Eds.), *Functional morphology of the vertebrates* (pp. 113–121). New York: Gustav Fischer.

Vassilieva, A. B. (2017). Heterochronies in the cranial development of Asian tree frogs (Amphibia: Anura: Rhacophoridae) with different life histories. *Doklady Biological Sciences, 473,* 50–52.

Vassilieva, A. B., Lai, J. S., Yang, S. F., Chang, Y. H., & Poyarkov Jr., N. A. (2015). Development of the bony skeleton in the Taiwan salamander, *Hynobius formosanus* Maki, 1922 (Caudata: Hynobiidae): heterochronies and reductions. *Vertebrate Zoology, 65,* 117–130.

Vera Candioti, M. F., Ubeda, C., & Lavilla, E. O. (2005). Morphology and metamorphosis of *Eupsophus calcaratus* tadpoles (Anura: Leptodactylidae). *Journal of Morphology, 264,* 161–177.

Vera Candioti, M. F., Nuñez, J. J., & Ubeda, C. (2011). Development of the nidicolous tadpoles of *Eupsophus emiliopugini* (Anura: Cycloramphidae) until metamorphosis, with comments on systematic relationships of the species and its endotrophic developmental mode. *Acta Zoologica, 92,* 27–45.

Wake, M. H., & Hanken, J. (1982). Development of the skull of *Dermophis mexicanus* (Amphibia: Gymnophiona), with comments on skull kinesis and amphibian relationships. *Journal of Morphology, 173,* 203–223.

Wassersug, R. J. (1976). A procedure for differential staining of cartilage and bone in whole formalin fixed vertebrates. *Stain Technology, 51,* 131–134.

Weisbecker, V., & Mitgutsch, C. (2010). A large-scale survey of heterochrony in anuran cranial ossification patterns. *Journal of Zoological Systematics and Evolutionary Research, 48,* 332–347.

Wiens, J. J. (1989). Ontogeny of the skeleton of *Spea bombifrons* (Anura: Pelobatidae). *Journal of Morphology, 202,* 29–51.

Yeh, J. (2002a). The evolution of development: two portraits of skull ossification in pipoid frogs. *Evolution, 56,* 2484–2498.

Yeh, J. (2002b). The effect of miniaturized body size on skeletal morphology in frogs. *Evolution, 56,* 628–641.

Ziermann, J. M., & Diogo, R. (2013). Cranial muscle development in frogs with different developmental modes: direct development versus biphasic development. *Journal of Morphology, 275,* 398–413.